

Electronic Theses and Dissertations, 2020-

2020

Water Reclamation Using Functionalized Forward Osmosis Membrane

Fnu Joshua
University of Central Florida

 Part of the [Environmental Engineering Commons](#)
Find similar works at: <https://stars.library.ucf.edu/etd2020>
University of Central Florida Libraries <http://library.ucf.edu>

This Masters Thesis (Open Access) is brought to you for free and open access by STARS. It has been accepted for inclusion in Electronic Theses and Dissertations, 2020- by an authorized administrator of STARS. For more information, please contact STARS@ucf.edu.

STARS Citation

Joshua, Fnu, "Water Reclamation Using Functionalized Forward Osmosis Membrane" (2020). *Electronic Theses and Dissertations, 2020-*. 444.
<https://stars.library.ucf.edu/etd2020/444>

WATER RECLAMATION USING FUNCTIONALIZED FORWARD OSMOSIS
MEMBRANE

By

FNU JOSHUA
S.Si Universitas Sumatera Utara, 2015

A thesis submitted in partial fulfillment of the requirements
for the degree of Master of Science in Environmental Engineering
in the Department of Civil, Environmental, and Construction Engineering
in the College of Engineering and Computer Science
at the University of Central Florida
Orlando, Florida

Spring Term
2020

Major Professor: A H M Anwar Sadmani

©2020 Joshua

ABSTRACT

This study investigated water reclamation from an impaired-quality water using forward osmosis (FO) membrane functionalized by nano zero valent iron (nZVI) loaded polyelectrolyte multilayer films. Stormwater runoff was selected as the impaired-quality water, which served as a feed solution (FS) and a NaCl salt solution at a concentration representing reverse osmosis (RO) concentrate was used as a draw solution (DS). RO concentrate is another impaired-quality water that is discharged to the environment with little or no treatment. A commercial cellulose triacetate (CTA) FO membrane was modified using poly allylamine hydrochloride (PAH) (a polycation) and poly acrylic acid (PAA) (a polyanion) following a dip coating method. In-situ synthesis of nZVI within the PAA/PAH layers was conducted through sodium borohydride reduction. The efficiency of the nZVI-PAA/PAH functionalized FO membranes in removing selected stormwater derived contaminants was evaluated.

The virgin CTA membrane had a rough surface and repeated applications of coatings were required to ensure uniform layers of PAA/PAH. Following 4, 8, 12, and 14 'bilayer' (BL) coatings, it was deduced that 14 BL coatings resulted in the most uniform layers with maximum surface coverage. The scanning electron microscopy (SEM) images demonstrated that the membrane coverage and uniformity of coating improved as more BL coatings were applied. While the unmodified membrane initially had a high flux ($16 \text{ L/m}^2\cdot\text{h}$) compared to the modified membranes, there was a sharp decline in flux (approximately $1.5 \text{ L/m}^2\cdot\text{h}$) within the first 2 to 3 h of operation, likely due to a rapid accumulation of foulants on the membrane surface. The modified membranes, on the other hand, showed markedly less initial flux ($2 \text{ L/m}^2\cdot\text{h}$), but the flux was maintained throughout the experimental period with only a slight decline. The flux decline that may be

anticipated owing to the additional layers on the membrane was probably offset by the hydrophilicity rendered by the PAA/PAH functional groups and less foulant accumulation.

The nZVI-loaded PAA/PAH coatings did not have any adverse impact on reverse salt flux (RSF). Any reduction in RSF due to the coatings might have been counteracted by the PAA/PAH induced dilution of the DS. While both NO_3^- and PO_4^{3-} removals were already very high (> 97%) when using the unmodified membrane, a slight increase in the removal of NO_3^- with increased BL numbers (8 and 14 BLs) was observed. The removal of selected heavy metals (Cd, Pb, and Cu) by the unmodified and modified membranes ranged from approximately 87% for Pb to almost complete (~99%) removal for Cd. Mass balance and energy dispersive x-ray spectroscopy (EDX) analyses confirmed that a higher number of coating resulted in a higher retention of heavy metals by the functionalized FO membranes. This could be attributed to the complexation of metal ions with carboxylate and amine groups from the PAA/PAH bilayers. Furthermore, the unmodified CTA FO membrane exhibited very high removal (> 97%) of perfluorooctanoic acid (PFOA) and perfluorooctanesulfonic acid (PFOS). EDX mapping showed that the 14 BL-nZVI membrane adsorbed more PFOS/A compared to the virgin and the 8 BL-nZVI membrane.

To my family and everyone who supported me. Thank you for all of your support.

ACKNOWLEDGMENTS

The research conducted in this thesis would not have been possible without the support of many individuals. I would like to thank Dr. A H M Anwar Sadmani for providing me the opportunity to conduct this research and for his guidance. I would also like thank my committee members, Dr. Lei Zhai, and Dr. Woo Hyung Lee for their guidance completing this study. I would like to acknowledge the funding support from the United States Environmental Protection Agency P3 Program.

TABLE OF CONTENTS

LIST OF FIGURES	ix
LIST OF TABLES	xi
CHAPTER 1: INTRODUCTION	1
CHAPTER 2: LITERATURE REVIEW	4
Stormwater Runoff	4
Stormwater Runoff Management	4
Water Reclamation	6
Forward Osmosis in Water Treatment	6
Membrane Surface Functionalization using Polyelectrolytes	8
Nano Zero Valent Iron for Water Treatment	9
CHAPTER 3: MATERIALS AND METHODS	10
Materials	10
Stormwater Characterization	11
Membrane Functionalization	12
Membrane Characterization	14
Bench-Scale Forward Osmosis Setup	15
LC-MS/MS Method for Perfluorooctanoic Acid (PFOA) and Perfluorooctanesulfonic Acid (PFOS) Analysis	16
Solid Phase Extraction Protocol for PFAS Sample Analysis	18
CHAPTER 4: RESULTS AND DISCUSSION	19
Characterization of Functionalized FO Membrane	19
Effect on the Membrane Coating Stages on nZVI Immobilization	22

Effect of Membrane Functionalization on FO Flux Performance.....	25
Effect on the Membrane Functionalization on the Solute Flux	26
Membrane Functionalization Effect for Nutrient Removal	29
Effect of Membrane Functionalization on Heavy Metal Removal	30
Removal of PFAS using Virgin and Modified FO Membranes.....	35
CHAPTER 5: CONCLUSIONS AND RECOMMENDATIONS.....	37
Conclusion.....	37
Recommendation.....	38
LIST OF REFERENCES	39

LIST OF FIGURES

Figure 1. Urban stormwater management practices based on their specificity and primary focuses [12].	5
Figure 2. Illustration of forward osmosis processes.	7
Table 2. Synthetic stormwater runoff composition.	12
Figure 3. Customized dip coating setup for applying polyelectrolyte layers on the membrane.	14
Figure 4. Bench-scale forward osmosis setup.	15
Table 3. SRM masses of PFOA and PFOS.	17
Figure 5. Scanning electron microscopy image of the unmodified CTA FO membrane.	19
Figure 6. Illustration of the membrane coating mechanism.	20
Figure 7. SEM images of functionalized FO membranes coated with 4 BL (a), 8 BL (b), 12 BL (c), and 14 BL (d) of PAH and PAA.	21
Figure 8. Illustration of membrane surface modification stages during dip coating.	22
Figure 9. SEM image (a) and EDX mapping of Fe (b) on 14 BL coated FO membrane.	23
Figure 10. Illustration of nZVI immobilization in 8 BL and 14 BL coated membrane substrates.	24
Figure 11. FO membrane flux from feed side to the draw solution side over a duration of 24 h.	25
Figure 12. Reverse Salt Flux of the Virgin, 8 BL-nZVI, and 14 BL-nZVI.	27
Figure 13. Stabilized RSF by the unmodified, 8BL-nZVI, and 14 BL-nZVI membranes.	28
Figure 16. Heavy metal removal mechanism by the modified membranes.	31
Figure 17. SEM images of the unmodified membrane and corresponding EDX mapping for, Cd (b), Cu (c), and Pb (d).	32

Figure 18. SEM images of the 8 BL-nZVI membrane and corresponding EDX mapping for, Cd (b), Cu (c), and Pb (d). 33

Figure 19. SEM images of the 14 BL-nZVI membrane and corresponding EDX mapping for, Cd (b), Cu (c), and Pb (d). 34

Figure 21. SEM images and their corresponding EDX mapping for F-elements for (a-b) virgin, (c-d) 8BL-nZVI, and (e-f) 14BL-nZVI membranes. 36

LIST OF TABLES

Table 1. Common parameters and equations used in FO processes.	7
Table 2. Synthetic stormwater runoff composition.....	12
Table 3. SRM masses of PFOA and PFOS.....	17
Table 4. Iron content in 8 and 14 BL coatings with respect to carbon	23
Table 5. Heavy metal adsorption by unmodified and modified FO membranes	33

CHAPTER 1: INTRODUCTION

Stormwater runoff is a major non-point source of pollution of surface and groundwater resources. Stormwater runoff accrues organic and inorganic contaminants including debris, pesticides, hydrocarbons, sediments, nutrients, and heavy metals such as Pb, Cd, Cu, Ni, Cr, and Zn. About 15% of impaired river miles in the US can be attributed to the discharge of stormwater [1, 2]. Approximately 11% of the EPA-assessed stream miles in the US are threatened or impaired due to excessive nutrient loading on the surface waters [1]. Various Best Management Practices (BMPs) are employed to control the anthropogenic pollution from stormwater runoff. Commonly used structural BMPs include wet and dry ponds, surface and underground sand filters, infiltration basins and trenches, and permeable pavements [3]. However, the removal of target nutrients, trace metals, and organic micropollutants when using BMPs is highly variable.

As the sources of freshwater continues to decrease, water reuse and reclamation have been of great interest in many parts of the world, including the US, in the recent decades. The waters reclaimed from stormwater can augment the supply of freshwater and can be used for potable or non-potable purposes including toilet flushing, irrigation, industrial usage, etc. Brackish water is another impaired-quality source that is utilized to produce potable water using brackish water reverse osmosis (BWRO). BWRO plants typically operate from 50 – 85 % recovery ranges, hence, 15 to 50% of the feedwater becomes concentrated brine [4]. Typical BWRO concentrates contain approximately 20,000 ppm of total dissolved solids; therefore, it will require very high pressure to purify it further due to its high osmotic pressure.

Forward osmosis (FO) is a membrane technology that utilizes the differences of osmotic pressure between a feed solution (FS) and a draw solution (DS) separated by a semi-permeable membrane. The yields of the FO treatment are diluted DS and concentrated FS. The FO membrane

processes can achieve similar organic rejection as the reverse osmosis (RO) processes [5]. Since FO does not require additional pressure to operate, it is an cost-efficient option compared to RO. However, some challenges associated with FO treatment for water reclamation include internal concentration polarization, reverse salt diffusion, and membrane fouling. To mitigate such problems, the FO membranes are suggested to be thin and smooth and possess hydrophilic and antimicrobial properties. There is a lack of studies exploring the reclamation of stormwater using FO technology.

This research is focused on treating an impaired-quality water using a modified FO membrane. Stormwater was reclaimed by utilizing simulated BWRO concentrate as the DS in a bench-scale FO system. In an attempt to overcome the drawbacks associated with the commercially available FO membranes, the membranes were functionalized by layer-by-layer depositing of polyelectrolyte multi-layer films (PMFs) and embedding zero valent iron nanoparticles (nZVIs) within the PMFs. Polyacrylic acid (PAA) and polyallylamine hydrochloride (PAH) were the polyelectrolytes selected for this purpose. nZVIs are generally used as environmental remediation substances because they demonstrate high reducing and absorption capacities for organics, heavy metals, and metalloid [6]. Therefore, FO membranes with embedded nZVIs in the active layer are expected to offer better removal of organic and inorganic contaminants while ensure adequate water flux.

The specific objectives of this research are:

- 1) To functionalize a commercial FO membrane using nZVI loaded PAA/PAH layers following a dip coating method;
- 2) To determine the effect of nZVI-PAA/PAH functionalization on membrane characteristics and flux performance;
- 3) To determine the effect of nZVI-integrated PAA/PAH multilayer films on the removal of nutrients, selected metals, and selected organic contaminants from synthetic stormwater runoff when using FO.

CHAPTER 2: LITERATURE REVIEW

Stormwater Runoff

Stormwater runoff can be considered as a source of a range of inorganic and organic pollutants including contaminants of emerging concern. The carried pollutants could be in form of chemical and biological contaminants that could possibly damage the aquatic ecosystems and cause adverse effects on human health [7]. Between 1991 to 2000, there had been more than 100 documented waterborne illness outbreaks in the US that were connected to the pathogens from the drinking water outbreaks [8]. Statistical studies on the US outbreak from 1949 to 1994 suggested that such outbreaks happened when there was a major rainfall. Those extreme events generated heavy stormwater runoff that eventually contaminated surface and groundwater resources [9]. Studies have been conducted for years to quantify the contaminants in the stormwaters such as, heavy metals, organics, nutrients [10], and per-and polyfluoroalkyl substances (PFAS) [11]. As a major non-point source pollution, the management of the stormwater is important in order to avoid the consequences of the stormwater derived pollutants.

Stormwater Runoff Management

Various best management practices (BMPs) are employed to mitigate the pollution from the stormwater runoff (Figure 1) [12]. Typically, two categories of BMPs, nonstructural BMPs (source control) and structural BMPs (retention, detention, and filtration) are applied. Commonly used structural BMPs include wet and dry ponds, surface and underground sand filters, infiltration basins and trenches, and permeable pavements [3]. Several studies [13-15] have investigated the performances of conventional urban stormwater runoff treatment systems; however focused mainly on the removal of trace metals and nutrients. Enhanced solid and nutrient removals were

observed when using bio-treatment systems incorporating depth filtration, sorption, precipitation, and ion exchange [16]. Limited studies [17, 18] have demonstrated or suggested the application of stormwater runoff–reclaimed water in irrigation purposes. Other management practices include providing public educations, encouraging the public involvement, illicit discharge detection and elimination, controlling the construction site, and post-construction control.

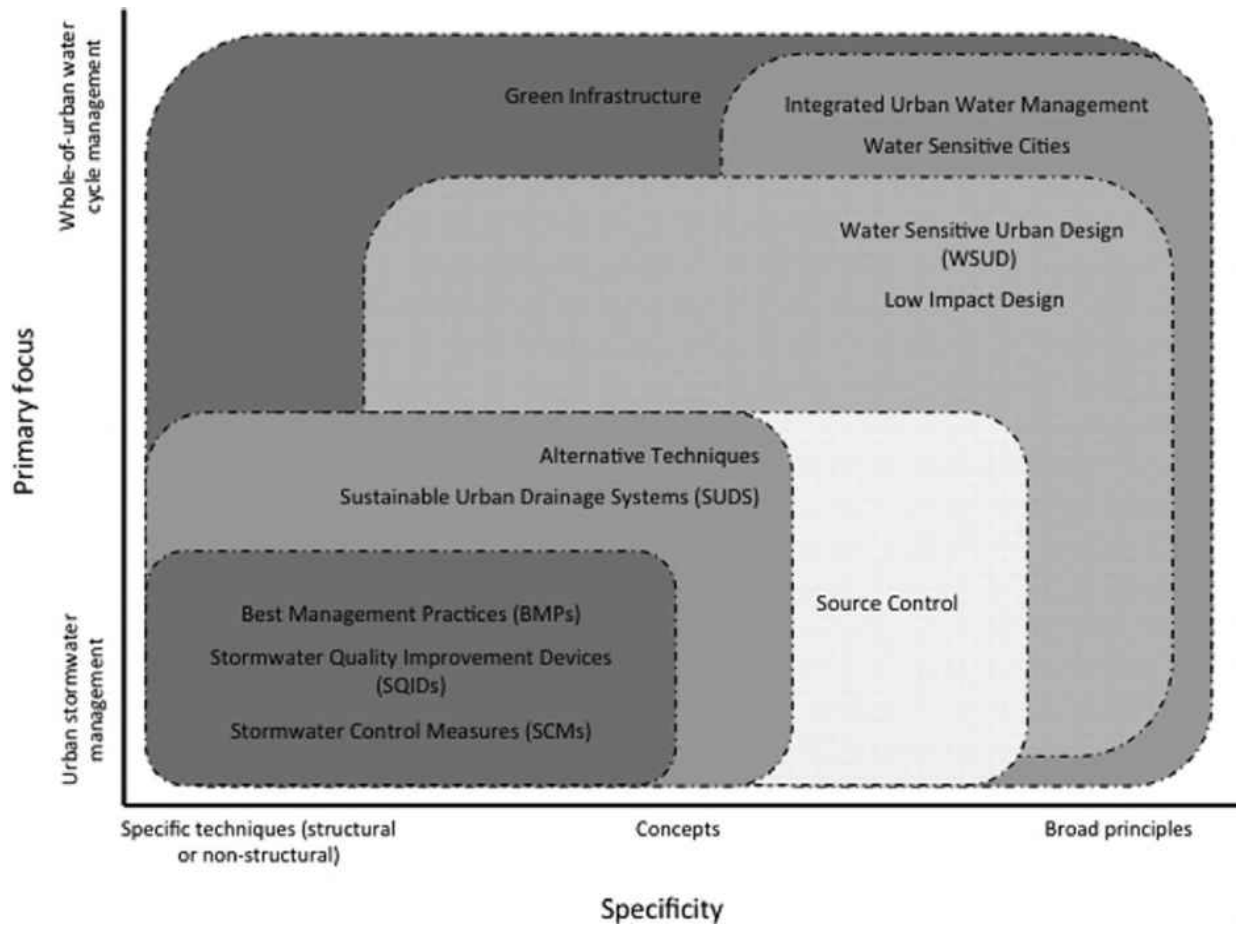


Figure 1. Urban stormwater management practices based on their specificity and primary focuses [12].

Water Reclamation

Water is the most essential commodity on earth; however, only 3% of the available water is freshwater. Because of population increment, the water usages have increased by six-fold in the 20th century [19]. The objective of the water reclamation is to achieve sustainability in water usage. Several arid countries in Asia and the Middle East are employing various water reclamation technologies due to the shortage of their water resources [20]. The reclaimed water generally contain high concentration of various ions, heavy metals, and organic compounds [21], but the qualities of the reclaimed waters depend on the local standards. In addition to other contaminants of emerging concern, per- and polyfluoroalkyl substances (PFAS) were reported in reclaimed waters [22]. Nutrients like nitrate and phosphate are also found in reclaimed waters and hence, the mismanagement of the reclaimed water could cause nutrient imbalances in the water ecosystems [23].

Forward Osmosis in Water Treatment

Forward Osmosis (FO) or osmotically driven membrane processes uses osmotic pressure as the main driving force to treatment water. Osmosis is the process of movement of water across a semi-permeable membrane due to the difference in osmotic pressure between two solutions. FO has been investigated to treat industrial wastewaters, landfill leachate, liquid food, and for water reclamation, and desalination [24]. As shown in Figure 2, FO process utilizes two different solutions: feed solution (FS) and draw solution (DS), having lower and higher osmotic pressures, respectively. FO performances depend on several membrane parameters including water permeability (A value), salt rejection (B value), and structural parameter (K value) (Table 1).

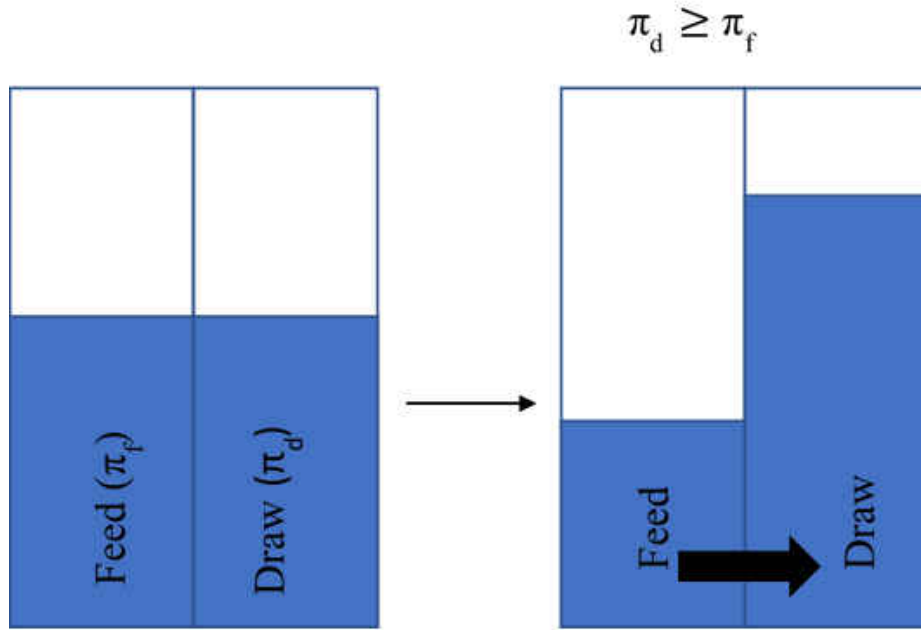


Figure 2. Illustration of forward osmosis processes.

Table 1. Common parameters and equations used in FO processes.

Parameters	Equations	Common Units	References
Water flux (J_w)	$J_w = A(\pi_D - \pi_F)$	$L \cdot m^{-2} \cdot h$ (LMH)	[25], [26]
Solute flux (J_s)	$J_s = B\Delta C$	$G \cdot m^{-2} \cdot h$ (GMH)	[25], [26]
Membrane structural parameter (K)	$K = \frac{t\tau}{D\varepsilon}$	mm^2/s	[25], [26]

There are two operational modes for FO: active layer facing draw solution (AL-DS) or active layer facing feed solution (AL-FS). Based on the operation mode, there are two different types of the internal concentration polarization (ICP). Dilutive ICP will be observed when the active layer faces FS and concentrative ICP will be observed when the active layer faces DS. Although FO operates at low or no applied pressure, the membrane is still subjected to fouling. Membrane fouling is the main challenge of all types of membrane processes. Membrane fouling reduces the fluid permeability of the membrane [27]. The origin and the mechanism of the membrane fouling is hard to predict because there are numerous factors that could affect membrane fouling. Several efforts had been made to reduce the membrane fouling, such as using material with low-fouling qualities, optimizing the operational conditions, etc [28].

Membrane Surface Functionalization using Polyelectrolytes

One of the methods to reduce membrane fouling is to modify the surface characteristics of the membrane. Majority of the foulants can attach to the surface of the membrane by adsorption caused by hydrophobic attraction, hydrogen bonding, van der Waals attraction, or electrostatic attraction [29]. The proper surface modification can mitigate all of the interactions resulting in a lower chance of membrane to become fouled. The membrane that has more hydrophilic surface is less prone to fouling [29, 30]. To address the fouling that is caused by the electrostatic attraction, the membrane should have the surface that has the similar charges to repel the treated contaminants [31]. The modification of membrane surface to increase the hydrophilicity and charge modification of the membrane active surface could be achieved by using polyelectrolyte coating [32].

The polyelectrolyte (PE) modification could be done by conformally depositing alternate PE charges, producing polyelectrolyte multi-layer films (PMFs) [33]. The coating can be applied using dip-coating, spin-coating, and spray coating [34]. The net charges of the coatings are dependent on the final layer of the coating. If the final layer of the coating is polyanion, the net charge of the surface will be negative and vice versa. PE coatings can provide anti-fouling properties to the membrane [35] due to the enhanced hydrophilicity and charge repulsion with the foulants. Several studies have shown that membranes modified via the application of PE coatings become resistant to fouling when compared to the unmodified membranes [35-37]. The PE layer-by-layer coating method could also be used as an approach for nanoparticles embedding [38].

Nano Zero Valent Iron for Water Treatment

Nanoparticles such as TiO₂ [39], Fe [40], Au [41], SnO₂ [42], and Ag [43] have been used as water remediation media as photocatalysts, or as anti-microbial agents. The nanoparticles are nanosized particles that have the particles size between 1 to 100 nm. Because of sizes of the nanoparticles, they are commonly more reactive than its bulk counterpart. Nanomaterials had been used to remove the heavy metals ion from the water [44]. Nanoscale metallic or zero valent iron (nZVI) has been demonstrated as an effective option to remove a wide variety of water contaminants including halogenated organic compounds, organophosphates, nitroamines and nitroaromatics, inorganic anions, heavy metals, metalloids, and actinides [45, 46].

CHAPTER 3: MATERIALS AND METHODS

Materials

Flat-sheet cellulose tri acetate (CTA) forward osmosis (FO) membranes were procured from Sterlitech (FTSH₂O, Sterlitech, Kent, WA, USA). All solutions used in this study were prepared using deionized water. Polyacrylic acid (PAA, 25% in water, M.W. 240,000) was purchased from ACROS Organics (Thermo Fisher, NJ, USA). Poly (allylamine hydrochloride) (PAH, M.W. 120,000 – 200,000) and sodium chloride (NaCl) were purchased from Alfa Aesar (Ward Hill, MA, USA). ACS grade sodium hydroxide (NaOH, pellet) and hydrochloric acid (HCl, 1 N) were purchased from Fisher Chemical (Thermo Fisher, NJ, USA). 2-(N-morpholino) ethane sulfonic acid (MES, fine white crystals) buffer was obtained from Fisher bioreagent (Thermo Fisher, NJ, USA) and 1-(3-Dimethylaminopropyl)-3-ethylcarbodiimide hydrochloride (EDC.HCl) was obtained from Advanced ChemTech (Louisville, KY, USA). Anhydrous ferric chloride (FeCl₃, 98%) was obtained from ACROS Organics (Thermo Fisher, NJ, USA). Sodium Borohydride (NaBH₄) was obtained from Fisher Chemical (Thermo Fisher, NJ, USA). Nitrate (10 mg/L NO₃⁻-N) and phosphate (1 mg/L PO₄³⁻) standards were obtained from Hach (Loveland, Colorado, USA). Nitrate testing kit (TNT plus 835, 0.23 – 13.5 mg/L NO₃⁻-N detection range) and phosphate testing kit (TNT plus 843, 0.15 – 4.5 mg/L PO₄³⁻ detection ranges) were obtained from Hach (Loveland, Colorado, USA). All bivalent heavy metal ion standards (1 mg/L; Cd, Cu, and Pb) were obtained from SPEX Certiprep (NJ, USA). Humic acid was obtained from Alfa Aesar (Ward Hill, MA, USA). Perfluorooctanoic acid (PFOA) and potassium perfluorooctanesulfonic acid (PFOS) were obtained from Sigma Aldrich (Millipore Sigma, Germany).

The solid phase extraction (SPE) was performed using weak anion exchange (WAX) mixed mode sorbent cartridges obtained from OASIS (3 cc, 30 μm , 60 mg, Waters (Milford, MA, USA)). All solution for the liquid chromatography tandem mass spectrometry analysis (LC-MS/MS) were prepared using LC-MS(Optima™) grade methanol and water (Thermo Fisher, NJ, USA). Optima™ grade formic acid (99%), ammonium acetate, and ammonium hydroxide were purchased from Fisher Chemical (Thermo Fisher, NJ, USA). A flat sheet FO testing cell CF-042A was procured from Sterlitech (Kent, WA, USA). The calibrated conductivity meter with auto-logging function was obtained from Apera Instruments (EC-820, Germany). The mass changes from the feed and draw solution were recorded by using auto-logging enabled scale connected to a computer.

Stormwater Characterization

Synthetic stormwater runoff was prepared in lab by spiking selected metals (Cu, Cd, Pb), nutrients, organics, and humic acid (Table 2). Humic acid was spiked as the representative of natural organic matter. To represent contaminants of emerging concern, perfluorooctanoic acid (PFOA) and perfluorooctanesulfonic acid (PFOS) were spiked in the FS. PFOA and PFOS concentrations in FSs were analyzed by a SPE-LC-MS/MS method developed based on the EPA Method 537 Rev. 1.1 [47]. In addition to monitoring the basic water quality parameters (such as pH, conductivity, and temperature data), the water samples were analyzed using spectrophotometer (DR5000, Hach, USA) for nutrients. Metal ions were analyzed using an Atomic Absorption Spectroscopy (AAS, Perkin Elmer, USA). The draw solution was prepared by spiking 20 g/L NaCl into deionized water.

Table 2. Synthetic stormwater runoff composition.

Contaminants	Concentration
Humic Acid	5 mg/L
Nitrate	10 mg/L
Phosphate	1 mg/L
Pb ²⁺	1 mg/L
Cd ²⁺	1 mg/L
Cu ²⁺	1 mg/L
PFOA	1 µg/L
PFOS	1 µg/L

Membrane Functionalization

Electrostatic interaction between opposite charges lead to the formation of multilayer films on a substrate via the dip coating method [34]. When dip coating is conducted using PE complexes, it is important to select the appropriate PE that is to be applied first. A previous study [48] reported the zeta potential (ξ) of CTA FO membranes to be -10 mV (at pH = 7.5), signifying the membranes have negatively-charged surfaces. Therefore, in the current study, PAH, was selected to be deposited on the membrane first, followed by PAA, which is a negatively charged PE.

A commercial CTA FO membrane was first rinsed by DI water and was immersed for 5 days in DI water. The membrane is preserved by 1% sodium metabisulfite solution by the manufacturer before shipping. The rinsing was conducted to ensure there were no residual of the sodium metabisulfite on the surface of the membrane active layer that could hinder the coating

process. The membrane was cut into a smaller piece to fit into the customized dip coating apparatus (Figure 3). The coating apparatus was designed such that only the active layer was exposed during the dip coating process.

The deposition process began by pouring 0.01 M PAH in 0.01 M of NaCl solution onto the dip coating apparatus. After 20 minutes, the coating solution was removed and was rinsed twice with DI water for 5 min each time to remove any residual NaCl and PAH. This was followed by immersing the membrane in 0.01 M PAA solution in 0.01 M NaCl for 20 min and rinsing twice with DI water for 5 min each time. These steps produced one 'bilayer' of PAH/PAA. This process was repeated to obtain the desired number of bilayers.

The coated membrane was soaked in 0.01 M of FeCl_3 solution for 30 min to form an iron-complex with carboxylic acid of the PAA, followed by rinsing with DI water to remove the excess FeCl_3 . Then, the membrane was soaked in 0.01 M of NaBH_4 solution for 10 min to reduce the complexed iron (III) to nano zero valent iron (nZVI) nanoparticles. To increase the amount of the nZVI on the coated membrane surface, the same protocol was repeated for four times. After the nZVI immobilization, the coated membrane was soaked in 1-ethyl-3-(3-dimethylaminopropyl) carbodiimide hydrochloride (EDC) and 2-(N-Morpholino)-ethanesulfonic acid (MES) buffer at pH 5.5 for one hour for crosslinking. The crosslinking was performed at pH 5.5 to optimize the process [49]. The virgin membrane was functionalized using 4, 8, 12, 14 nZVI-loaded PAA/PAH bilayer.



Figure 3. Customized dip coating setup for applying polyelectrolyte layers on the membrane.

Membrane Characterization

The surface and cross-sections of membrane samples were examined by field emission scanning electron microscopy (FE-SEM) (ZEISS, Gemini Ultra 55, USA). Energy dispersive x-Ray spectroscopy (EDS) was used to determine the elements within the membrane coatings. The membrane cross-sections were prepared by snapping the membrane inside a liquid nitrogen bath. All membrane surface sample was sputter coated by gold for ~5 nm thickness and the images were obtained using around 4.5 mm working distances and 5 keV accelerating voltages.

Bench-Scale Forward Osmosis Setup

A bench-scale FO system, as shown in Figure 4, was used to determine the water flux performance and the removal of nutrients, selected metals, and selected organic contaminants from stormwater using unmodified and modified FO. The experimental setup consisted of FO membrane test cells, feed and draw delivery pumps, two scales connected to the computer to auto-log the mass for every 1.5 minutes, a calibrated conductivity meter with auto-logging function to measure the conductivity of the feed solution, and two containers for the feed and draw solutions.



Figure 4. Bench-scale forward osmosis setup.

The feed and the draw solution were pumped by a peristaltic pump with a flow rate of 4 mL/h. The membrane active surface area of the cell is 42 cm². The calibrated conductivity meter with auto-log function was used to measure the conductivity differences for every 15 min throughout the experiments. Before running the experiments, the system was equilibrated using DI water for at-least 24 h. After 24-h, the feed and draw solutions were added to the respective tanks. The samples for the contaminant removal analysis were taken before and after the treatment.

The water flux of the experiment was calculated using the following Equation 1.

$$J_w = \frac{\Delta m}{A \cdot \Delta t \cdot \rho_w} \quad (1)$$

Where Δm is the mass changes in the solutions, A is the membrane active area, Δt is the time difference, and ρ_w is the density of water at 22 °C, and

$$J_s = \frac{(C_t V_t - C_0 V_0)}{A \cdot t} \quad (2)$$

Where C_0 and C_t are the concentrations of the feed solution at time 0 and t , respectively; V_0 and V_t are the volumes of the feed solution at time 0 and t , respectively.

LC-MS/MS Method for Perfluorooctanoic Acid (PFOA) and Perfluorooctanesulfonic Acid (PFOS) Analysis

An Accucore™ C18 2.6 μm 80 \AA 100 mm x 2.1 mm (ThermoFisher Scientific, NJ, USA) separation column was used for the analysis. 10 mM ammonium acetate prepared using LC-MS grade water was used as the mobile phase ‘A’ and LC-MS grade methanol as the mobile phase ‘B’. All mobile phases were degassed by sonicating the solution for 15 min. The high-performance liquid chromatography pump used for the analysis was Ultimate 3000 pump (ThermoScientific, NJ, USA), operated at a flow rate of 0.1 mL/min. The pump gradient for the method was 0-3 min, 40% B; 3-5.5 min, 40%-95.5% B; 5.5-12 min, 95.5% B; 12-12.1 min, 95.5%-100% B; 12.1 -14 min, 100% B; 14 – 14.1 min, 100%- 40% B; 14.1- 18 min, 40% B, ‘end’. The temperature of the column was set at 30 °C. The volume of the sample injection was 5 μL .

The triple quadrupole mass spectrometer TSQ Quantum Access Max (ThermoScientific, NJ, USA) was used as the mass detector. The detection was performed in negative mode using a

heated electrospray ionizer (H-ESI) and the analysis was performed using selected reaction monitoring (SRM) mode. The software used to control the analysis was Tracefinder™ (Version 3.2, ThermoScientific, NJ, USA). The ion spray voltage was set to 2800 V, the capillary temperature was set to 270 °C, and the sheath gas pressure was 15 psi. The collision gas used was Argon with 1.5 mTorr collision gas pressure. The SRM masses investigated are summarized in Table 3. The calibration standard of the analysis was prepared using 1, 5, 10, 25, 50, 75, 100, 125, and 150 ng/ml of PFOA and PFOS standards. All of the standards were prepared using LC-MS grade methanol. The PFOA stock solution was prepared using 96:4 methanol/water solvent, and the PFOS stock solution was prepared using LC-MS grade methanol. The method detection limit (MDL) was 4 ng/ L for both PFOA and PFOS.

Table 3. SRM masses of PFOA and PFOS.

Compounds	Parent Ion Mass (Q ₁ , m/z)	Product Ion Mass (Q ₃ , m/z)
Perfluorooctanoic Acid (PFOA)	413	170
Perfluorooctanoic Acid (PFOA)	413	369
Perfluorooctanesulfonic Acid (PFOS)	499	99
Perfluorooctanesulfonic Acid (PFOS)	499	80

Solid Phase Extraction Protocol for PFAS Sample Analysis

The PFOA and PFOS in feed and draw solutions before and after 24-h filtration were extracted using Oasis WAX cartridges. Before loading the samples onto the SPE cartridges, the samples were acidified using hydrochloric acid 1 N to bring the pH of the solution to 3. The solid phase extraction (SPE) protocol used a 20-position vacuum extraction manifold (Agilent, USA). The extraction was initiated by conditioning the cartridges using 2 ml of the LC-MS grade methanol, followed by 2 ml LC-MS grade water. After the cartridges were conditioned, 20 ml of the previously acidified sample was added with a flow rate of 0.6 ml/min. Then, the cartridges were washed by 1 ml of 2% formic acid in LC-MS water solution. The samples were eluted by using 500 μL (2 x 250 μL) LC-MS grade methanol and 500 μL (2 x 250 μL) 5% ammonium hydroxide solution in LC-MS grade methanol. The eluted samples were then dried using a nitrogen evaporator at 65-67 °C. The dried samples were reconstituted using 400 μL of 96:4 methanol/water solution in 2 ml autosampler vials with polypropylene insert spring and polypropylene caps. Both PFOA and PFOS recoveries using the SPE method were $70 \pm 5\%$.

CHAPTER 4: RESULTS AND DISCUSSION

Characterization of Functionalized FO Membrane

The CTA FO membrane selected for this study has a slightly rough surface as shown in the scanning electron microscopy (SEM) image in Figure 4. The membrane underwent several surface modifications stages as a result of systematic application of a number of coating layers (Figure 6). The coating was initiated by immersing the FO membrane substrate onto a positively charged PAH solution. The PAH molecules in the dipping solution slowly accumulated and precipitated on the surface of the FO membrane (which has a negatively charged surface) due to electrostatic attraction between the membrane substrate and PAH.

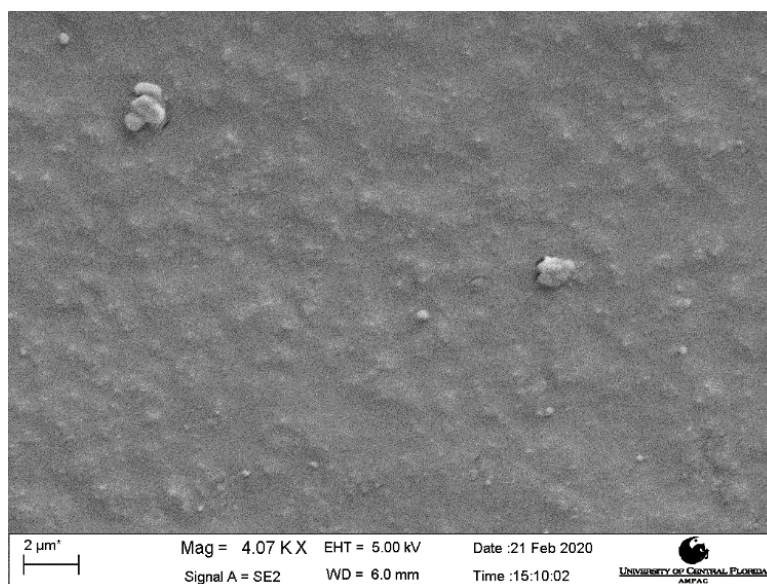


Figure 5. Scanning electron microscopy image of the unmodified CTA FO membrane.

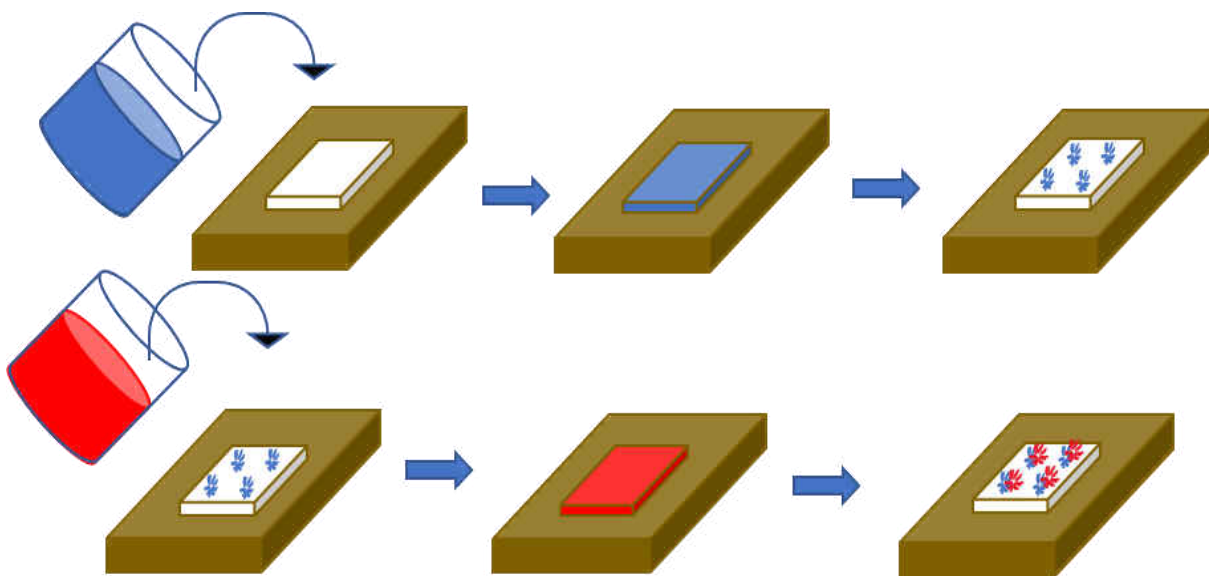


Figure 6. Illustration of the membrane coating mechanism.

Because of the roughness of the virgin membrane substrate (Figure 5), repeated application of coating was required to ensure uniform layers of PEs. Accordingly, 4, 8, 12, and 14 ‘bilayer’ (BL) coatings were deposited on the membrane surface and examined using FE-SEM. Figure 7 (a) shows the SEM image of the membrane after 4 BL coating. During this stage (i.e., the stage of 4 BL coating), the coating was observed to be rather unevenly distributed over the surface area of the membrane. After 8 BL coating (Figure 7 (b)) more coverage forming spiderweb-like layers was observed. This indicated that more bilayer applications should lead to more uniformity of the deposition. As shown in Figure 7 (c), the deposition of 12 BLs results in more coverage with relatively more uniform when compared to the 8 BL- coated. Finally, 14 BL coating showed even more coverage (Figure 7(d) compared to the 4 and 8 BL coatings.

This demonstrates that there is a clear link between the number of bilayers deposited and coverage and uniformity of PE coating. The coating number, however, must be optimized with respect to the flux loss and contaminant rejection by the functionalized membrane. Figure 8 is an illustration of different stages of membrane surface modification using dip coating.

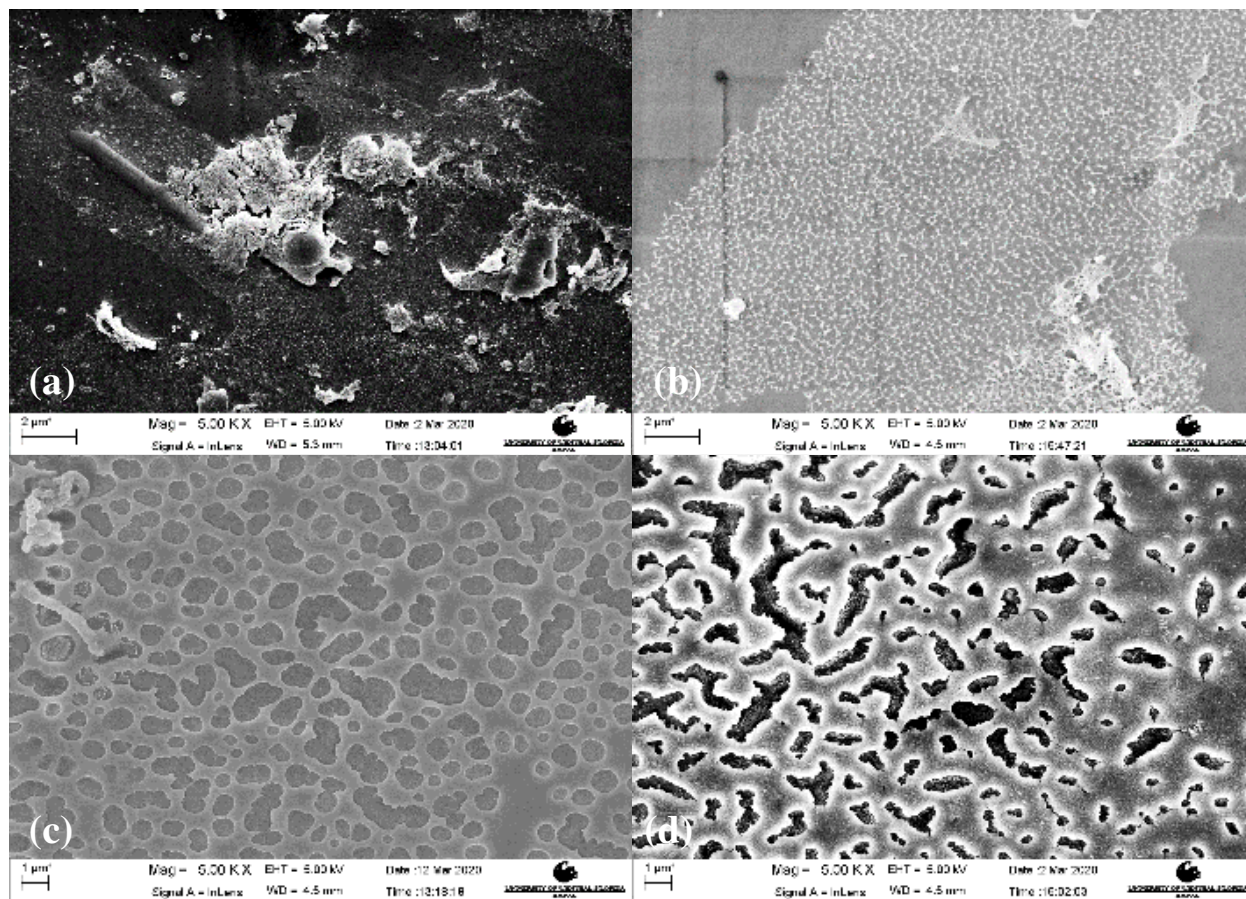


Figure 7. SEM images of functionalized FO membranes coated with 4 BL (a), 8 BL (b), 12 BL (c), and 14 BL (d) of PAH and PAA.

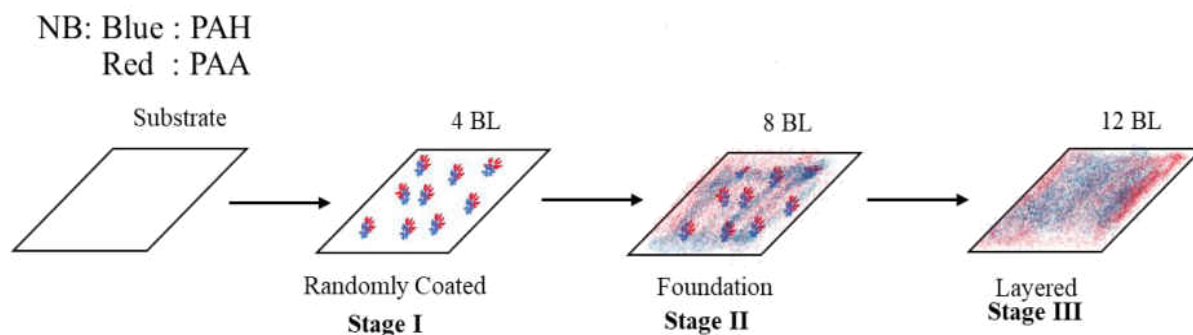


Figure 8. Illustration of membrane surface modification stages during dip coating.

Effect on the Membrane Coating Stages on nZVI Immobilization

Energy dispersive x-ray spectroscopy (EDX) analysis was used to study the relationship between the number of bilayer coating application and the amount of nZVI immobilized on the membrane (within the PE coatings). Figure 9 (a) shows the SEM image of the FO membrane coated the 14 BLs and Figure 9 (b) shows the EDX mapping of iron (Fe) on the FO membrane. It can be inferred from Figure 8 that Fe was distributed uniformly on the surface of the membrane when nZVI were immobilized with the crosslinked PE bilayers. When the polyelectrolyte complex (PEC) bilayers are immersed into the FeCl_3 solution during membrane functionalization, the carboxylate ($-\text{COO}^-$) groups from PAA form complexes with Fe^{3+} [50], which are reduced to nZVI (Fe^0) when immersed in a NaBH_4 solution. Thus, the availability of carboxylate groups plays an important role in nZVI immobilization. The percentages of Fe with respect to carbon in 8 and 14 BL coated membranes, as obtained from EDX, are shown in Table 4. This observation indicates that a higher number of PE bilayer coatings result in higher amount of nZVI immobilization on the membrane surface. A schematic of nZVI immobilization in 8 BL and 14 BL coated membrane substrate is presented in Figure 10.

Table 4. Iron content in 8 and 14 BL coatings with respect to carbon

Atomic Ratio Percentage	PE bilayer-coated FO membranes	
	8 Bilayers	14 Bilayers
% (Fe/C)	1.4834	3.2764

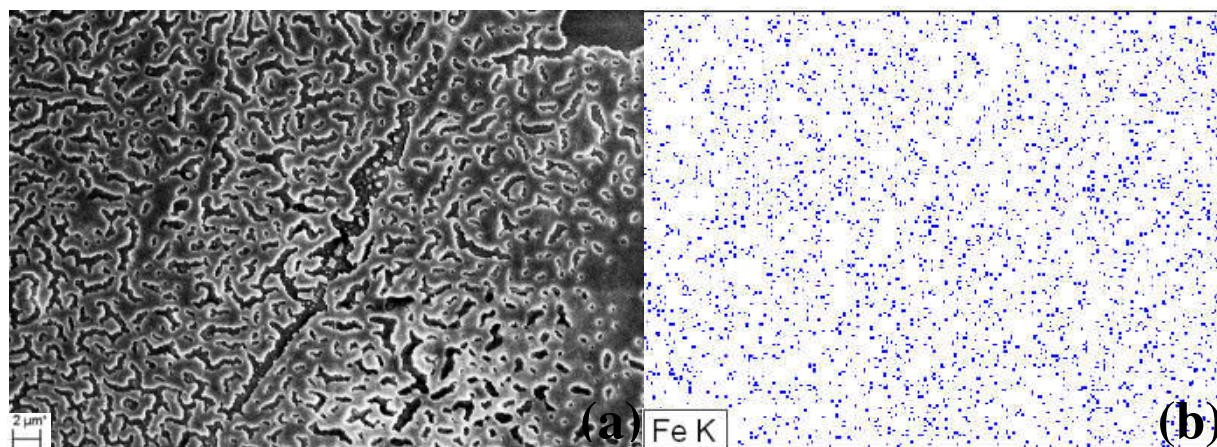


Figure 9. SEM image (a) and EDX mapping of Fe (b) on 14 BL coated FO membrane.

Blue : PAH
 Red : PAA
 Yellow : Iron (III) ion
 Black : nZVI
 Grey raster : Crosslinking by EDC

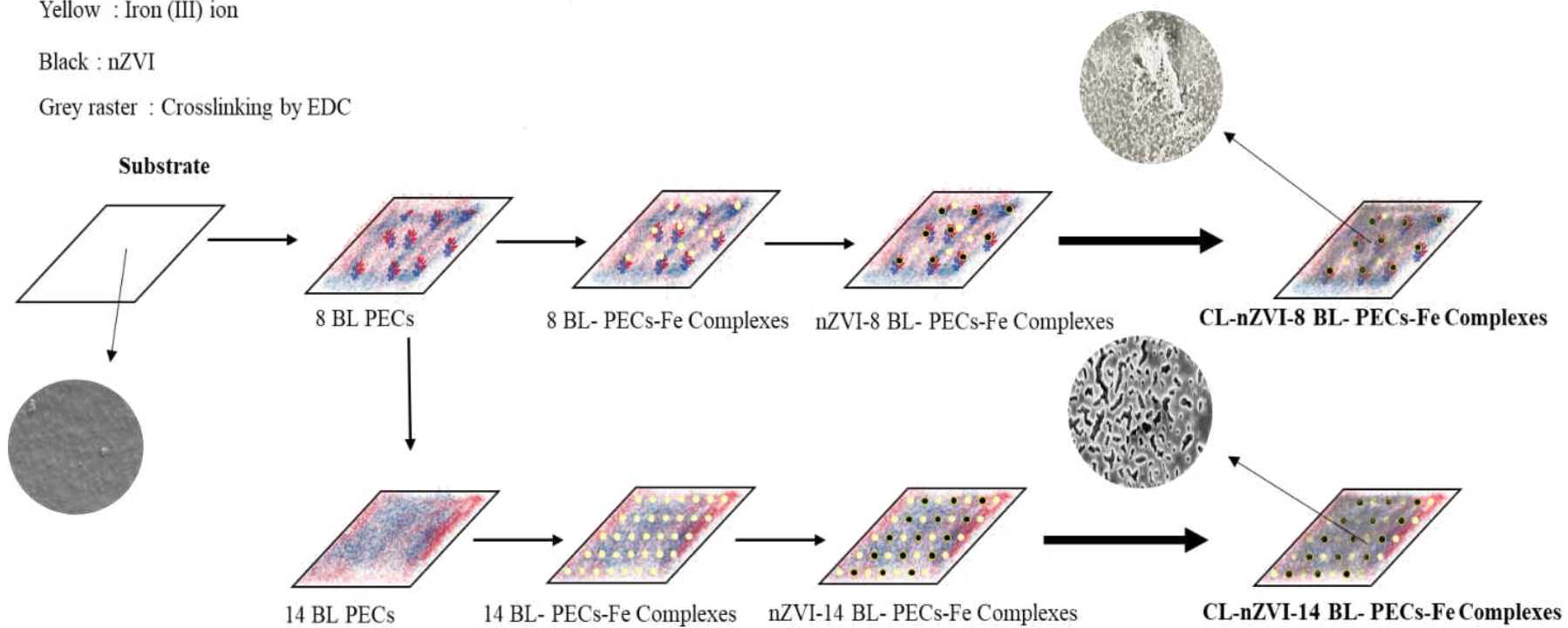


Figure 10. Illustration of nZVI immobilization in 8 BL and 14 BL coated membrane substrates.

Effect of Membrane Functionalization on FO Flux Performance

The flux performance of the functionalized FO membrane was compared to that of the unmodified membrane. Figure 11 presents the FO membrane flux from the feed side to the draw solution side over a duration of 24 h. The virgin membrane, as expected, commenced with a high flux (1.6 L/m².h) after stabilization, but exhibited a sharp decline after 4 h, likely due to a rapid accumulation of foulants on the surface (feed side). While the 8 BL coated-nZVI loaded membrane (BL-nZVI) showed a stable initial flux (1.4 L/m².h), no appreciable decline in flux was observed during the experimental period. Contrarily, the 14 BL-nZVI membrane initially produced negligible flux; however, interestingly, the flux was increased to approximately 1.4 L/m².h after 10 h and was sustained at around 1.5 L/m².h for the rest of the experimental duration.

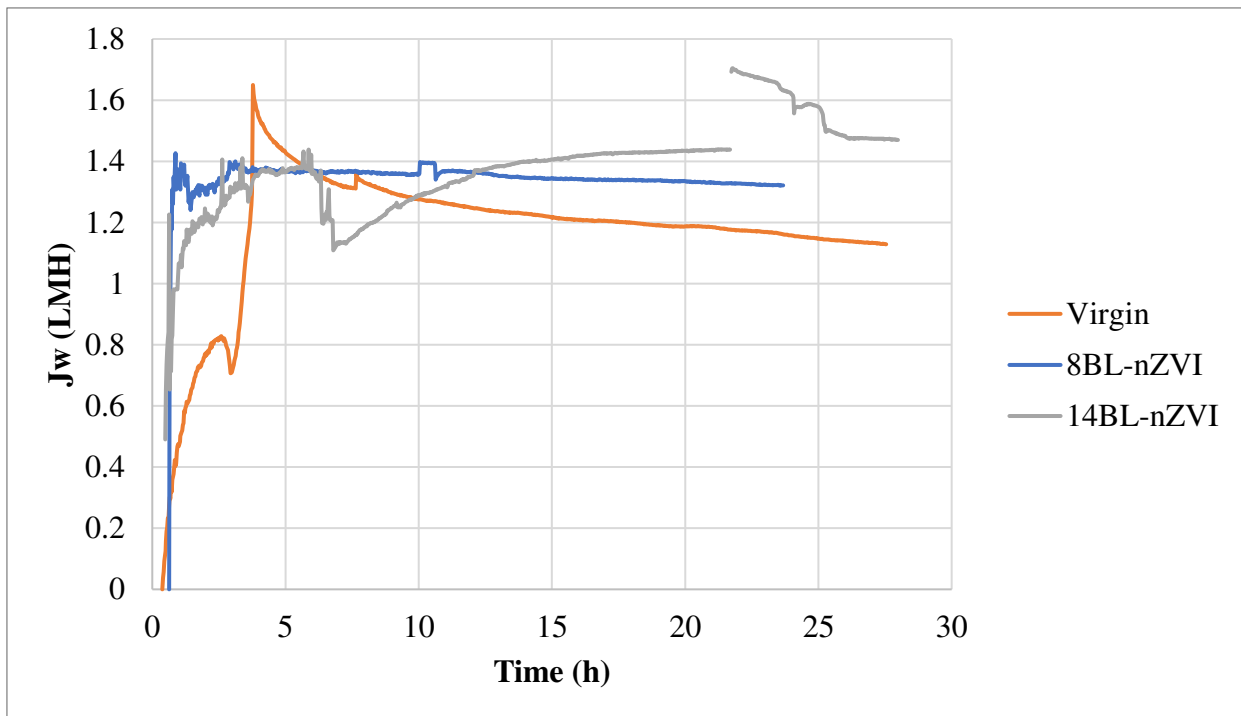


Figure 11. FO membrane flux from feed side to the draw solution side over a duration of 24 h.

One would anticipate that the deposition of additional layers on a membrane substrate would cause a membrane flux decline. However, it is known that hydrophilicity plays an important role in membrane flux performance. Hydrophilic membranes are less fouling prone [51] and less affected by concentration polarization [52]. PE and nZVI functionalization are expected to render the CTA FO membrane more hydrophilic when compared to the virgin membrane owing to the surface chemistry of deposited materials.

The virgin membrane has a smoother surface compared to the modified membranes. The sharp decline of the feed flux is probably due to the dilutive internal concentration polarization (ICP). CTA membrane has moderate hydrophilicity because of the hydrogen bonding from its acetic bond. Upon PAH/PAA functionalization, the carboxylic acid (-COOH) and the amine (-NH₂) groups likely facilitate more hydrogen bonding.

Hence, the modified membranes are expected to become more hydrophilic with increasing number of PAH/PAA layers. The flux decline for the coated membrane over time was likely offset by the increased hydrophilicity of the membranes and due to less accumulation of foulants. The 14 BL-nZVI membrane, which produced apparently no flux at the beginning due to the 14 bilayers of the PAH/PAA, exhibited increased flux in approximately 4 h due to hydrophilicity imparted by the PAH/PAA layers.

Effect on the Membrane Functionalization on the Solute Flux

Reverse salt flux (RSF) is a major drawback associated with FO processes. (RSF) is the diffusion of salt from the DS to the FS. Since the driving force of the FO processes is the osmotic pressure difference between the FS and the DS. If the salt ions from the DS diffuse to the FS, the water flux will be eventually reduced. RSF is expected to be more significant when the FO process is operated

in active layer (AL)-FS mode because the DS face the ‘loose’ support layer of the membrane. RSF during FO operation using the virgin and the 8 and 14 BL-nZVI membrane, is shown in Figure 12. As expected, the RSF is initially high because DS contain a high concentration of salt. The RSF decreases with time since the DS become diluted and the FS becomes concentrated, lowering the diffusion of salt from the DS to the FS. From Figure 12, it appears that the membrane functionalization using nZVI-loaded PAH/PAA coatings did not have any adverse impact on the RSF. Any reduction in RSF due to the coatings might have been counteracted by the PAH/PAA induced dilution of the DS.

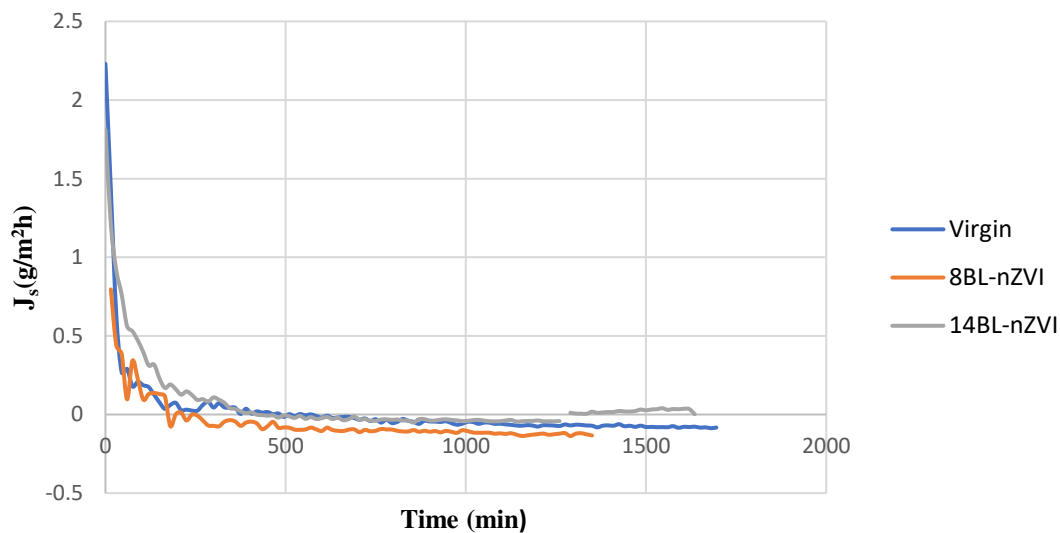


Figure 12. Reverse Salt Flux of the Virgin, 8 BL-nZVI, and 14 BL-nZVI

Another major drawback in FO processes is membrane fouling, which is generally caused by the accelerated cake-enhanced osmotic pressure (A-CEOP) that can be triggered by the RSF [53]. Figure 13 shows the average reverse salt flux (RSF) by the unmodified and modified membranes after the fluxes became stabilized. Hence, this data represents the RSF conditions when the foulants have accumulated on the membrane surface. Under this condition, the 14 BL-nZVI

exhibited the lowest RSF compared to the unmodified and 8 BL-nZVI membranes. This could be because this membrane has more PAA/PAH layers providing hydrophilicity and these additional layers increased the tortuosity for the salt to pass through to the feed side. The hydrophilicity counteracted the effect of dilutive ICP. However, there is a small increment in RSF by the 8BL-nZVI membrane, probably due to the dilutive ICP from the active layer side.

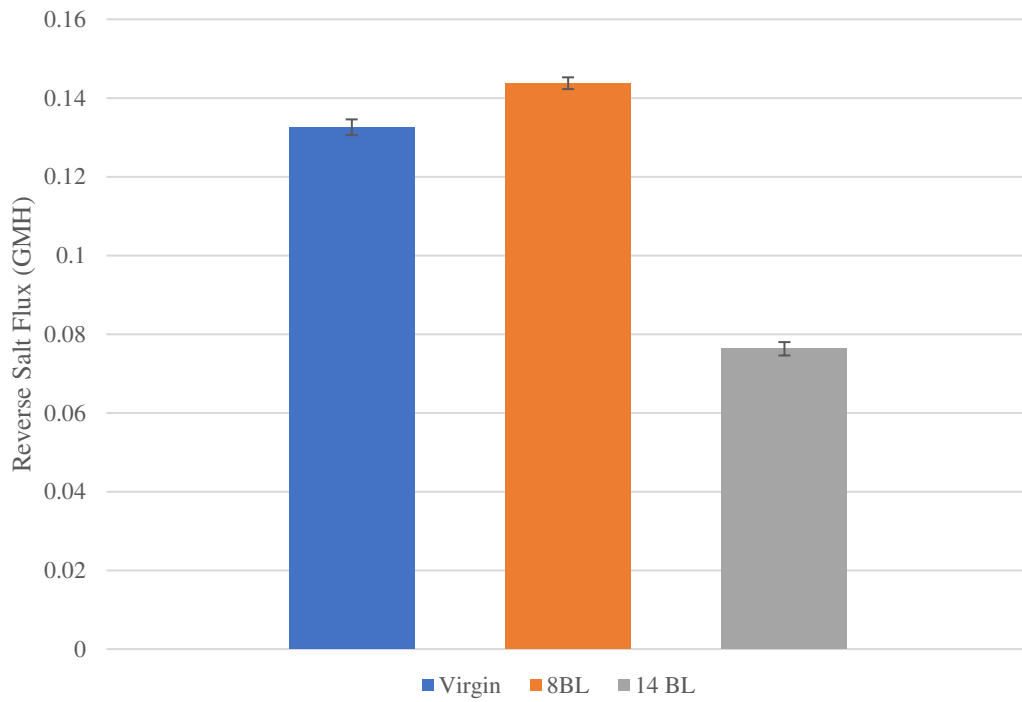


Figure 13. Stabilized RSF by the unmodified, 8BL-nZVI, and 14 BL-nZVI membranes

Membrane Functionalization Effect on Nutrient Removal

Nitrate (NO_3^-) and phosphate (PO_4^{3-}) removals from the simulated stormwater runoff by the unmodified and functionalized FO membranes were tested using a bench-scale FO setup. The removals were estimated by comparing the nutrients' concentration in the FS (stormwater runoff) and DS. Figure 14 shows NO_3^- and PO_4^{3-} removal using the virgin, 8 BL-nZVI, and 14 BL-nZVI membranes. The virgin membrane showed almost complete removal of PO_4^{3-} and the modified membranes maintained the same level of removal. While NO_3^- removal was also already very high (97.5%) by the virgin membrane, a slight increase in removal with increased BL numbers (8 and 14 BLs) was observed.

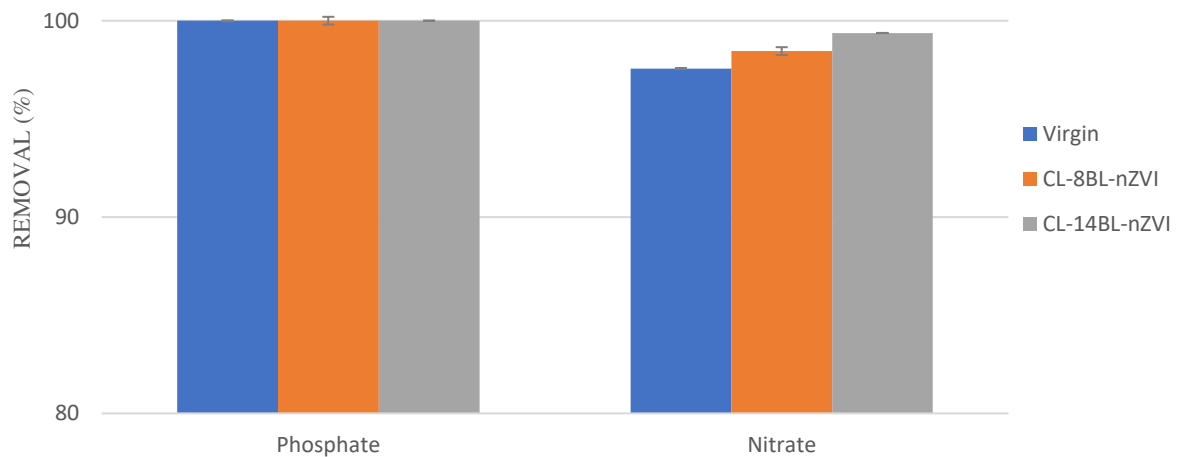


Figure 14. Nutrient removal using virgin, 8BL-nZVI, and 14BL-nZVI FO membranes

Effect of Membrane Functionalization on Heavy Metal Removal

The unmodified and modified FO membranes were tested for their heavy metal removal efficiency from stormwater runoff using NaCl as a DS. The removal of the selected heavy metals (Cd, Pb, and Cu) ranged from approximately 87% for Pb to almost complete (~99%) removal for Cd (Figure 15). There was an increasing trend of removal of the metals with the higher number of BLs when comparing 8 and 14 BL-coated membranes. The removal of Cd by the virgin membrane was already very high and the coated membranes showed a similar or a slightly higher removal. The removal of Pb increased from approximately 87% (virgin membrane) to approximately 95% when the membrane was coated with 14 BL PAH/PAA. A similar trend was observed for the removal of Cu, which increased from approximately 89% to approximately 94%.

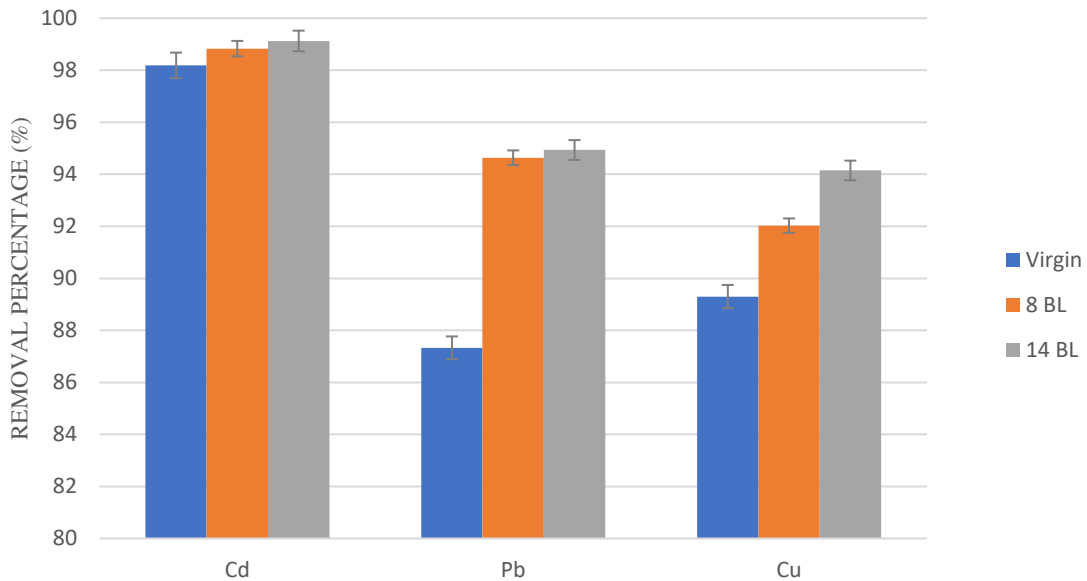


Figure 15. Heavy metal (Cd, Pb, and Cu) removal by the virgin and modified membranes.

The membrane modification introduced carboxylate and amine groups to the CTA surface of the FO membrane. The carboxylate group could bind with the divalent heavy metal atom and form a complex compound (Figure 16). This is plausible mechanism of enhanced metal removal by the PAH/PAA functionalized membranes when compared to the unmodified membrane.

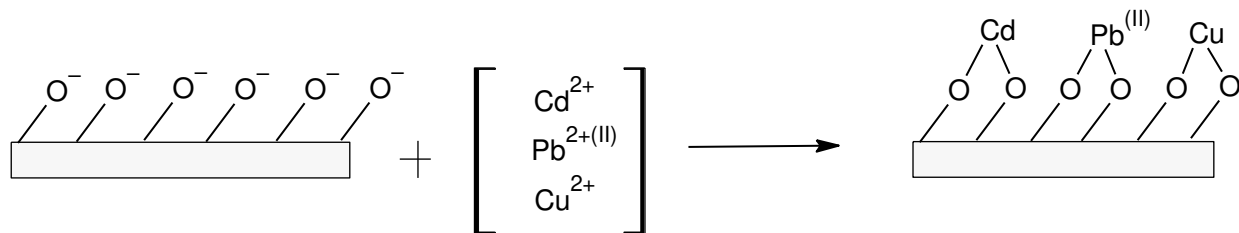


Figure 16. Heavy metal removal mechanism by the modified membranes.

If the metals form complexes with the carboxylate groups from the PAH/PAA coatings, it can be hypothesized that the mass adsorption of the heavy metals by the modified membranes should be higher compared to the virgin membrane. This can be tested by applying a simple mass balance on the metals in the FS. As shown in Table 5, the virgin membrane adsorbed only up to approximately 5% of the metals, likely due to the unacetylated cellulose of the membrane and the hydroxyl (-OH) groups from the cellulose forming complexes with heavy metals. The modified membrane showed more metal adsorption due to the presence of the carboxylate groups as discussed earlier. Up to 22% adsorption of Pb was estimated from the mass balance (Table 5) when using the 14 BL- nZVI membrane. The 14 BL-nZVI membrane, however, showed less Cd adsorption (~7%) probably because of the competition of Cd with Pb and Cu to form complexes.[54]

For further confirmation of the above finding, the unmodified and modified membranes were examined using EDX. Figure 17, 18, and 19 show the SEM images of the corresponding EDX

mapping for the tested heavy metals for the unmodified, 8BL-nZVI, and 14 BL-nZVI, respectively. The EDX maps indicate that the 14 BL-nZVI membrane had the highest amount of heavy metals on its surface, which is consistent with the finding based on the mass balance approach discussed before. Thus, it is confirmed that a higher number of coating results in a higher retention of heavy metals by the FO membrane.

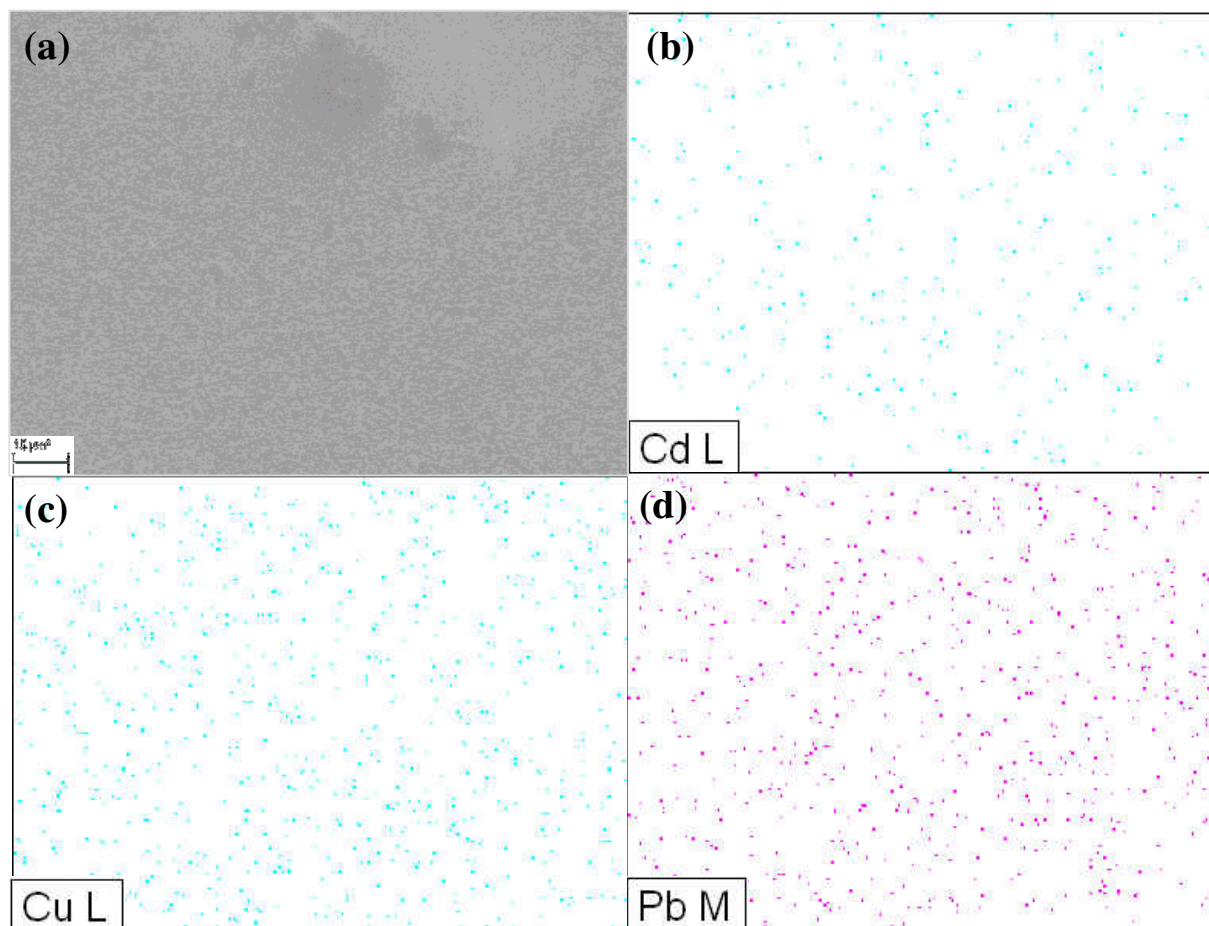


Figure 17. SEM images of the unmodified membrane and corresponding EDX mapping for, Cd (b), Cu (c), and Pb (d).

Table 5. Heavy metal adsorption by unmodified and modified FO membranes

Membrane	% Mass adsorbed		
	Cd	Pb	Cu
Virgin	3.337199	1.140278	4.841007
8BL-nZVI	11.90415	15.4	16.69758
14BL-nZVI	6.947018	22.08189	19.43209

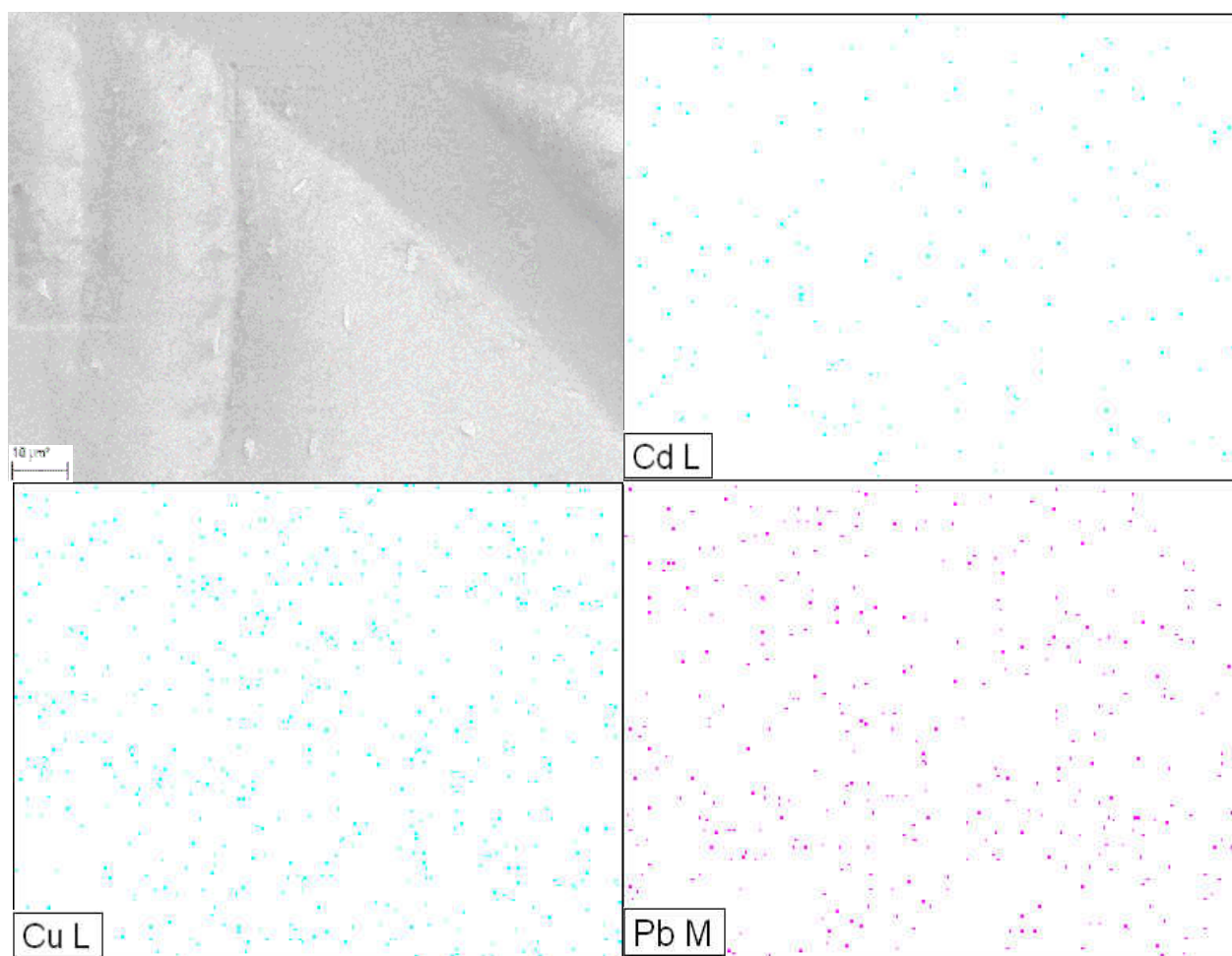


Figure 18. SEM images of the 8 BL-nZVI membrane and corresponding EDX mapping for, Cd (b), Cu (c), and Pb (d).

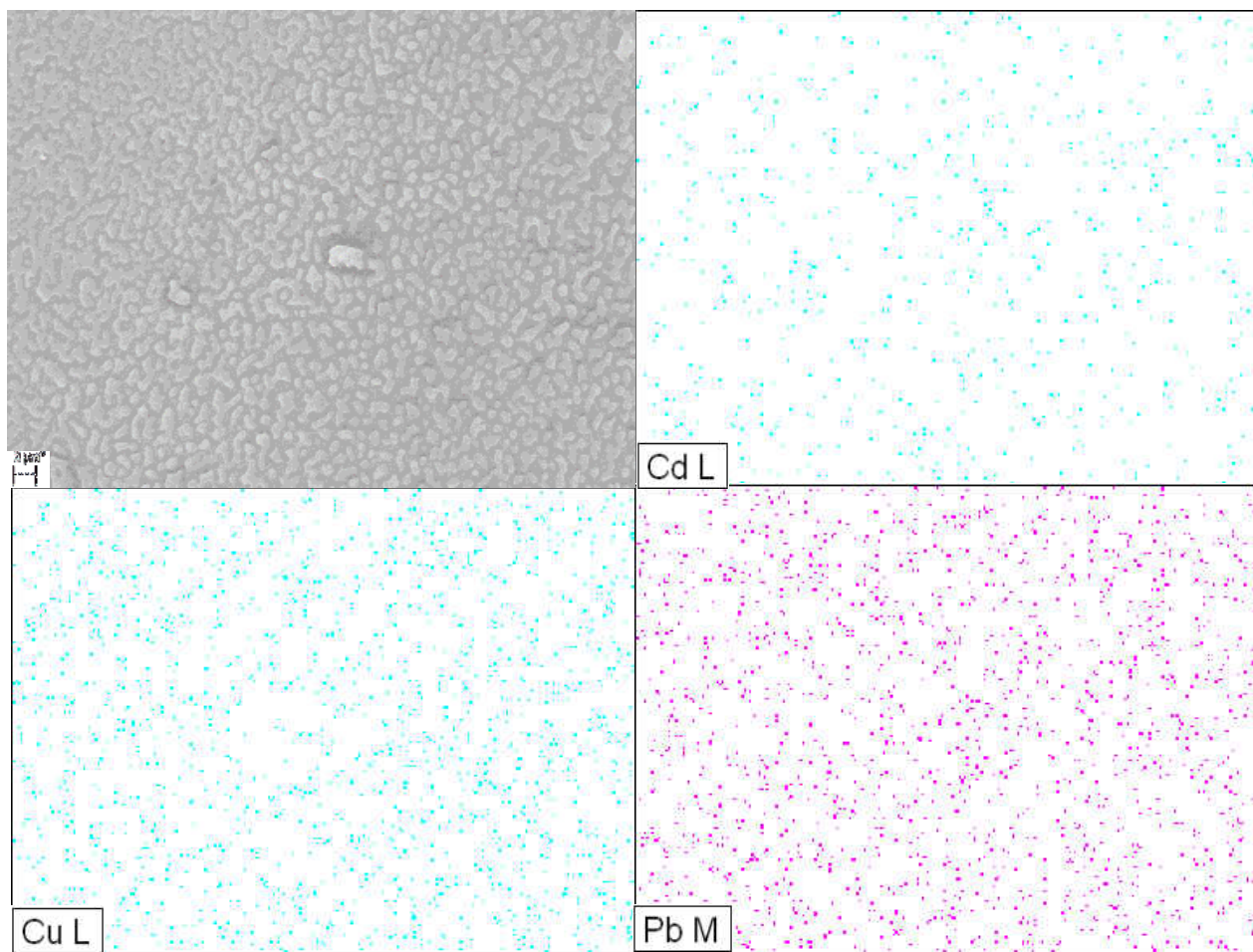


Figure 19. SEM images of the 14 BL-nZVI membrane and corresponding EDX mapping for, Cd (b), Cu (c), and Pb (d).

Removal of PFAS using Virgin and Modified FO Membranes

The unmodified CTA FO membrane exhibited very high removal of the selected PFASs. Approximately 97% PFOA and 98% PFOS (Figure 20) were removed by the virgin membrane. The presence of fluorine serves as an indicator of PFAS in a sample matrix and hence, the detection of total fluorine (TF) has been recently used as an approach for rapid screening of PFASs [50]. To confirm the adsorption of PFOS/A by the functionalized FO membranes, EDX analysis was conducted in this study. Figure 21 show the SEM Images and their corresponding EDX fluorine (F) mapping for virgin, 8 BL-nZVI, and 14 BL-nZVI membranes. The X-ray detection peaks for F (F K α) was clearly the highest for the 14 BL-nZVI membrane, indicating that this membrane adsorbed more PFOS/A compared to the virgin and the 8 BL-nZVI membrane.

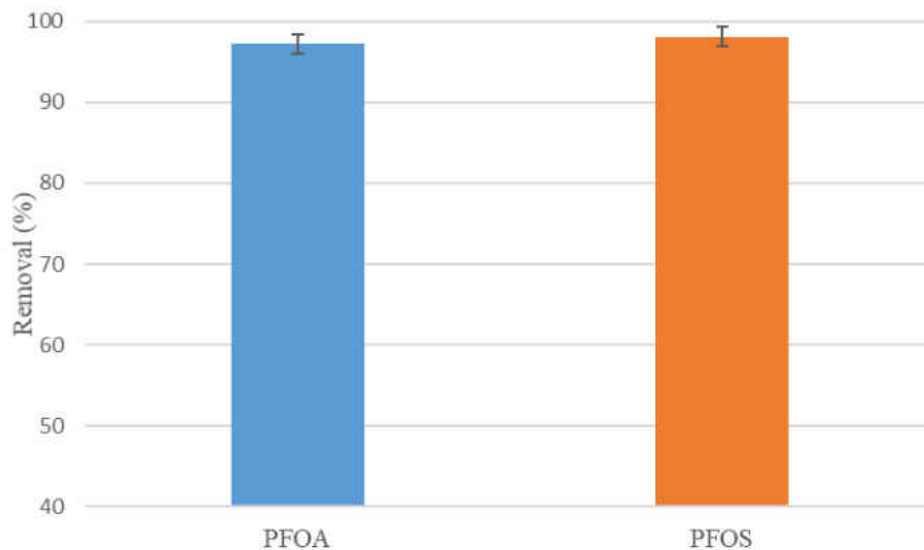


Figure 20. PFOA/S removal using virgin membrane.

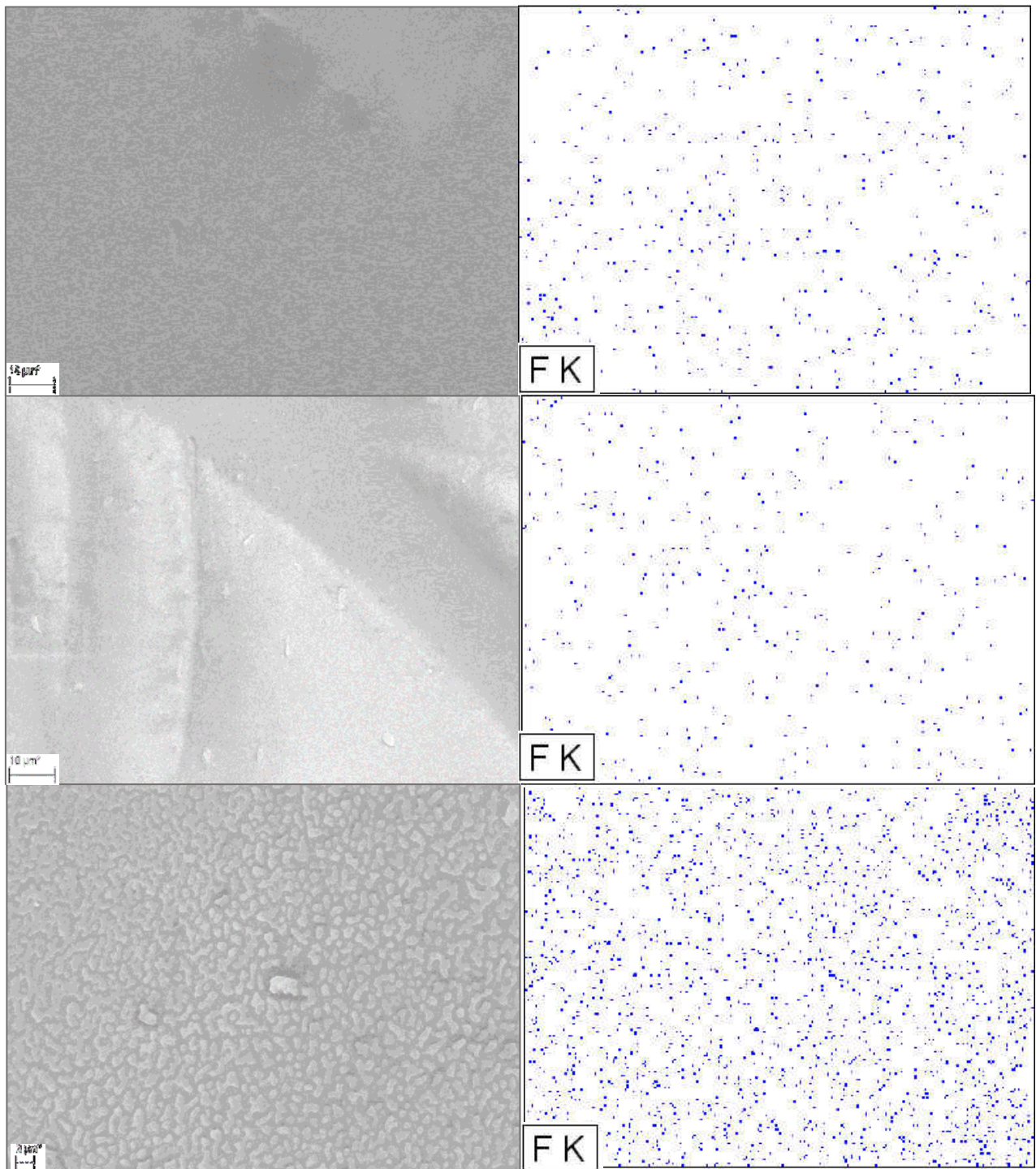


Figure 21. SEM images and their corresponding EDX mapping for F-elements for (a-b) virgin, (c-d) 8BL-nZVI, and (e-f) 14BL-nZVI membranes.

CHAPTER 5: CONCLUSION AND RECOMMENDATION

Conclusions

In this study, a commercially available CTA FO membrane was functionalized using PAA/PAH multilayer films with embedded nZVI to reclaim water from an impaired-quality source, stormwater runoff. Repeated applications of PAA/PAH 'bilayers' (BL) were required to ensure uniform coating of the rough CTA membrane surface active layer. The membrane coverage and uniformity of coating improved as more BL coatings were applied. In addition, SEM images indicated that a higher number of PAA/PAH bilayer coatings result in higher amount of nZVI immobilization on the membrane surface. The coating protocol, however, must be optimized with respect to the flux loss and contaminant rejection by the functionalized membrane. While the modified membranes showed markedly less initial flux compared to the unmodified membrane, the flux was maintained throughout the experimental period with only a slight decline. The flux decline was probably offset by hydrophilicity rendered by the PAA/PAH functional groups and less foulant accumulation. The nZVI-loaded PAA/PAH coatings did not have any adverse impact on reverse salt flux. While both NO_3^- and PO_4^{3-} removal was already very high when using the unmodified membrane, a slight increase in the removal of NO_3^- with increased BL numbers was observed. Mass balance and EDX analyses revealed that a higher number of coatings resulted in a higher retention of heavy metals by the functionalized FO membranes. This could be attributed to the complexation of metal ions with carboxylate and amine groups from the PAA/PAH bilayers deposited on the membrane. Although the unmodified membrane already showed very high removal of POFS and PFOA, more retention of these compounds can be expected if more bilayer coatings are applied.

This study suggested that the treatment of urban stormwater using the modified FO membrane can produce water that will be amenable to water reclamation purposes. The functionalized membrane efficiently removed nutrients, PFAS, and heavy metals. However, the final concentration of the draw solution, although diluted, may need further treatment before being reused. The bench-scale experiments were conducted using smaller membrane specimens. It is suggested that larger membrane coupons be used for future experiments to verify the impact of membrane area on draw solution salt concentration.

Recommendations

Water reclamation from other impaired-quality sources should be examined following the FO process developed in this study. Future work should focus on additional FO membrane coating methods using other PE complexes. Commercial FO membranes are produced by a limited number of manufacturers. Hence, future work should attempt fabricating FO membranes that can be fine-tuned for desired properties. FO membranes must be optimized for fouling resistance and reverse salt flux. The effects of additional water quality parameters on the FO process using the functionalized membranes should be determined. The effects of draw solution concentration and other FO operating conditions should be tested as well.

In this study, NaCl was added to the coating solution to improve the deposition rate of the polyelectrolytes. However, the experiments on the effect of the NaCl concentration on the membrane morphology were not performed due to the time constraint. Additional researches could be performed to study the effect of the NaCl on the morphology of the coated membrane. Furthermore, future research should study how to optimize further the immobilization of nZVI within the bilayer coatings.

LIST OF REFERENCES

- [1] USEPA, "National water quality inventory, 305(b) Report. EPA-841-R-02-001," US Environmental Protection Agency, Washington, DC, 2000.
- [2] M. A. Mallin, V. L. Johnson, and S. H. Ensign, "Comparative impacts of stormwater runoff on water quality of an urban, a suburban, and a rural stream," *Environmental Monitoring and Assessment*, journal article vol. 159, no. 1, pp. 475-491, 2008, doi: 10.1007/s10661-008-0644-4.
- [3] A. J. Erickson, P. T. Weiss, and J. S. Gulliver, *Optimizing Stormwater Treatment Practices: A Handbook of Assessment and Maintenance*. Springer New York, 2013.
- [4] P. Xu, T. Y. Cath, A. P. Robertson, M. Reinhard, J. O. Leckie, and J. E. Drewes, "Critical review of desalination concentrate management, treatment and beneficial use," *Environmental Engineering Science*, vol. 30, no. 8, pp. 502-514, 2013.
- [5] M. Xie, L. D. Nghiem, W. E. Price, and M. Elimelech, "Comparison of the removal of hydrophobic trace organic contaminants by forward osmosis and reverse osmosis," *Water research*, vol. 46, no. 8, pp. 2683-2692, 2012.
- [6] X. Zhao, W. Liu, Z. Cai, B. Han, T. Qian, and D. Zhao, "An overview of preparation and applications of stabilized zero-valent iron nanoparticles for soil and groundwater remediation," *Water research*, vol. 100, pp. 245-266, 2016.
- [7] R. Rangsviek and M. Jekel, "Removal of dissolved metals by zero-valent iron (ZVI): Kinetics, equilibria, processes and implications for stormwater runoff treatment," *Water Research*, vol. 39, no. 17, pp. 4153-4163, 2005.

- [8] S. J. Gaffield, R. L. Goo, L. A. Richards, and R. J. Jackson, "Public health effects of inadequately managed stormwater runoff," *American Journal of Public Health*, vol. 93, no. 9, pp. 1527-1533, 2003.
- [9] F. C. Curriero, J. A. Patz, J. B. Rose, and S. Lele, "The association between extreme precipitation and waterborne disease outbreaks in the United States, 1948–1994," *American journal of public health*, vol. 91, no. 8, pp. 1194-1199, 2001.
- [10] D. K. Makepeace, D. W. Smith, and S. J. Stanley, "Urban stormwater quality: summary of contaminant data," *Critical Reviews in Environmental Science and Technology*, vol. 25, no. 2, pp. 93-139, 1995.
- [11] E. Hepburn, C. Madden, D. Szabo, T. L. Coggan, B. Clarke, and M. Currell, "Contamination of groundwater with per-and polyfluoroalkyl substances (PFAS) from legacy landfills in an urban re-development precinct," *Environmental pollution*, vol. 248, pp. 101-113, 2019.
- [12] T. D. Fletcher *et al.*, "SUDS, LID, BMPs, WSUD and more – The evolution and application of terminology surrounding urban drainage," *Urban Water Journal*, vol. 12, no. 7, pp. 525-542, 2015/10/03 2015, doi: 10.1080/1573062X.2014.916314.
- [13] R. Berbee, G. Rijs, R. d. Brouwer, and L. v. Velzen, "Characterization and treatment of runoff from highways in the Netherlands paved with impervious and pervious asphalt," *Water Environment Research*, vol. 71, pp. 183-190, 1999.
- [14] K. Bratieres, T. D. Fletcher, A. Deletic, and Y. Zinger, "Nutrient and sediment removal by stormwater biofilters: A large-scale design optimisation study," *Water Research*, vol. 42, no. 14, pp. 3930-3940, 8// 2008, doi: <http://dx.doi.org/10.1016/j.watres.2008.06.009>.

- [15] A. P. Davis, M. Shokouhian, H. Sharma, C. Minami, and D. Winogradoff, "Water quality improvement through bioretention: lead, copper, and zinc removal," *Water Environment Research*, vol. 75, pp. 73-82, 2003.
- [16] M. Wanielista, M. Hardin, A. Hood, I. Gogo-Abite, and M. Chopra, "Stormwater Harvesting Using Retention and In-Line Pipes for Treatment Consistent with the new Statewide Stormwater Rule," 2013.
- [17] Z. Li, R. Valladares Linares, M. Abu-Ghdaib, T. Zhan, V. Yangali-Quintanilla, and G. Amy, "Osmotically driven membrane process for the management of urban runoff in coastal regions," *Water Research*, vol. 48, pp. 200-209, 1/1/ 2014, doi: <http://dx.doi.org/10.1016/j.watres.2013.09.028>.
- [18] D. Norton-Brandão, S. M. Scherrenberg, and J. B. van Lier, "Reclamation of used urban waters for irrigation purposes – A review of treatment technologies," *Journal of Environmental Management*, vol. 122, pp. 85-98, 6/15/ 2013, doi: <http://dx.doi.org/10.1016/j.jenvman.2013.03.012>.
- [19] F. R. Rijsberman, "Water scarcity: Fact or fiction?," *Agricultural Water Management*, vol. 80, no. 1, pp. 5-22, 2006/02/24/ 2006, doi: <https://doi.org/10.1016/j.agwat.2005.07.001>.
- [20] L. Yi, W. Jiao, X. Chen, and W. Chen, "An overview of reclaimed water reuse in China," *Journal of Environmental Sciences*, vol. 23, no. 10, pp. 1585-1593, 2011.
- [21] W. Chen, S. Lu, W. Jiao, M. Wang, and A. C. Chang, "Reclaimed water: A safe irrigation water source?," *Environmental Development*, vol. 8, pp. 74-83, 2013.

- [22] M. Murakami, H. Shinohara, and H. Takada, "Evaluation of wastewater and street runoff as sources of perfluorinated surfactants (PFSs)," *Chemosphere*, vol. 74, no. 4, pp. 487-493, 2009.
- [23] L. Candela, S. Fabregat, A. Josa, J. Suriol, N. Vigués, and J. Mas, "Assessment of soil and groundwater impacts by treated urban wastewater reuse. A case study: Application in a golf course (Girona, Spain)," *Science of the Total Environment*, vol. 374, no. 1, pp. 26-35, 2007.
- [24] T. Cath, "Osmotically and thermally driven membrane processes for enhancement of water recovery in desalination processes. *Desalin Water Treat* 15 (1–3): 279–286," ed, 2010.
- [25] D. L. Shaffer, J. R. Werber, H. Jaramillo, S. Lin, and M. Elimelech, "Forward osmosis: where are we now?," *Desalination*, vol. 356, pp. 271-284, 2015.
- [26] K. Lee, R. Baker, and H. Lonsdale, "Membranes for power generation by pressure-retarded osmosis," *Journal of membrane science*, vol. 8, no. 2, pp. 141-171, 1981.
- [27] H. Li and V. Chen, "Membrane fouling and cleaning in food and bioprocessing," in *Membrane Technology*: Elsevier, 2010, pp. 213-254.
- [28] Y. Chun, D. Mulcahy, L. Zou, and I. S. Kim, "A Short Review of Membrane Fouling in Forward Osmosis Processes," *Membranes*, vol. 7, no. 2, p. 30, 06/12
- [29] N. Hilal, O. O. Ogunbiyi, N. J. Miles, and R. Nigmatullin, "Methods employed for control of fouling in MF and UF membranes: a comprehensive review," *Separation Science and Technology*, vol. 40, no. 10, pp. 1957-2005, 2005.

- [30] M. Kabsch-Korbutowicz, K. Majewska-Nowak, and T. Winnicki, "Analysis of membrane fouling in the treatment of water solutions containing humic acids and mineral salts," *Desalination*, vol. 126, no. 1-3, pp. 179-185, 1999.
- [31] B. Van der Bruggen, M. Mänttari, and M. Nyström, "Drawbacks of applying nanofiltration and how to avoid them: a review," *Separation and purification technology*, vol. 63, no. 2, pp. 251-263, 2008.
- [32] C. Ba, D. A. Ladner, and J. Economy, "Using polyelectrolyte coatings to improve fouling resistance of a positively charged nanofiltration membrane," *Journal of Membrane Science*, vol. 347, no. 1-2, pp. 250-259, 2010.
- [33] M. L. Bruening, D. M. Dotzauer, P. Jain, L. Ouyang, and G. L. Baker, "Creation of functional membranes using polyelectrolyte multilayers and polymer brushes," *Langmuir*, vol. 24, no. 15, pp. 7663-7673, 2008.
- [34] N. Joseph, P. Ahmadiannamini, R. Hoogenboom, and I. F. Vankelecom, "Layer-by-layer preparation of polyelectrolyte multilayer membranes for separation," *Polymer Chemistry*, vol. 5, no. 6, pp. 1817-1831, 2014.
- [35] J. Wang, Y. Yao, Z. Yue, and J. Economy, "Preparation of polyelectrolyte multilayer films consisting of sulfonated poly (ether ether ketone) alternating with selected anionic layers," *Journal of Membrane Science*, vol. 337, no. 1-2, pp. 200-207, 2009.
- [36] M. Müller, T. Rieser, K. Lunkwitz, and J. Meier-Haack, "Polyelectrolyte complex layers: a promising concept for anti-fouling coatings verified by in-situ ATR-FTIR spectroscopy," *Macromolecular rapid communications*, vol. 20, no. 12, pp. 607-611, 1999.

- [37] M. Müller, T. Rieser, P. L. Dubin, and K. Lunkwitz, "Selective interaction between proteins and the outermost surface of polyelectrolyte multilayers: influence of the polyanion type, pH and salt," *Macromolecular rapid communications*, vol. 22, no. 6, pp. 390-395, 2001.
- [38] S. Srivastava and N. A. Kotov, "Composite layer-by-layer (LBL) assembly with inorganic nanoparticles and nanowires," *Accounts of chemical research*, vol. 41, no. 12, pp. 1831-1841, 2008.
- [39] S. O. Obare and G. J. Meyer, "Nanostructured materials for environmental remediation of organic contaminants in water," *Journal of Environmental Science and Health, Part A*, vol. 39, no. 10, pp. 2549-2582, 2004.
- [40] X.-q. Li, D. W. Elliott, and W.-x. Zhang, "Zero-valent iron nanoparticles for abatement of environmental pollutants: materials and engineering aspects," *Critical reviews in solid state and materials sciences*, vol. 31, no. 4, pp. 111-122, 2006.
- [41] R. Subair, B. P. Tripathi, P. Formanek, F. Simon, P. Uhlmann, and M. Stamm, "Polydopamine modified membranes with in situ synthesized gold nanoparticles for catalytic and environmental applications," *Chemical Engineering Journal*, vol. 295, pp. 358-369, 2016.
- [42] G. C. de Assis *et al.*, "Conversion of "Waste Plastic" into photocatalytic nanofoams for environmental remediation," *ACS applied materials & interfaces*, vol. 10, no. 9, pp. 8077-8085, 2018.
- [43] N. Ahmad and S. Sharma, "Green synthesis of silver nanoparticles using extracts of *Ananas comosus*," 2012.

- [44] S. Thatai, P. Khurana, J. Boken, S. Prasad, and D. Kumar, "Nanoparticles and core–shell nanocomposite based new generation water remediation materials and analytical techniques: A review," *Microchemical Journal*, vol. 116, pp. 62-76, 2014.
- [45] R. A. Crane and T. B. Scott, "Nanoscale zero-valent iron: Future prospects for an emerging water treatment technology," *Journal of Hazardous Materials*, vol. 211–212, pp. 112-125, 4/15/ 2012, doi: <http://dx.doi.org/10.1016/j.jhazmat.2011.11.073>.
- [46] H.-J. Lu, J.-K. Wang, S. Ferguson, T. Wang, Y. Bao, and H.-x. Hao, "Mechanism, synthesis and modification of nano zerovalent iron in water treatment," *Nanoscale*, 10.1039/C6NR00740F vol. 8, no. 19, pp. 9962-9975, 2016, doi: 10.1039/C6NR00740F.
- [47] J. Shoemaker, "Method 537. Determination of selected perfluorinated alkyl acids in drinking water by solid phase extraction and liquid chromatography/tandem mass spectrometry (LC/MS/MS)," 2009.
- [48] X. Jin, J. Shan, C. Wang, J. Wei, and C. Y. Tang, "Rejection of pharmaceuticals by forward osmosis membranes," *Journal of hazardous materials*, vol. 227, pp. 55-61, 2012.
- [49] P. F. Gratzer and J. M. Lee, "Control of pH alters the type of cross-linking produced by 1-ethyl-3-(3-dimethylaminopropyl)-carbodiimide (EDC) treatment of acellular matrix vascular grafts," *Journal of Biomedical Materials Research: An Official Journal of The Society for Biomaterials, The Japanese Society for Biomaterials, and The Australian Society for Biomaterials and the Korean Society for Biomaterials*, vol. 58, no. 2, pp. 172-179, 2001.
- [50] L. Schultes *et al.*, "Total Fluorine Measurements in Food Packaging: How Do Current Methods Perform?," *Environmental Science & Technology Letters*, vol. 6, no. 2, pp. 73-78, 2019.

- [51] W. Yang *et al.*, "The effect of wetting property on anti-fouling/foul-release performance under quasi-static/hydrodynamic conditions," *Progress in Organic Coatings*, vol. 95, pp. 64-71, 2016.
- [52] N. Saxena, C. Prabhavathy, S. De, and S. DasGupta, "Flux enhancement by argon–oxygen plasma treatment of polyethersulfone membranes," *Separation and purification technology*, vol. 70, no. 2, pp. 160-165, 2009.
- [53] S. Lee, C. Boo, M. Elimelech, and S. Hong, "Comparison of fouling behavior in forward osmosis (FO) and reverse osmosis (RO)," *Journal of membrane science*, vol. 365, no. 1-2, pp. 34-39, 2010.
- [54] A. Denizli, B. Garipcan, A. Karabakan, R. Say, S. Emir, and S. Patir, "Metal-complexing ligand methacryloylamidocysteine containing polymer beads for Cd (II) removal," *Separation and purification technology*, vol. 30, no. 1, pp. 3-10, 2003.